A diffusion-controlled mullite formation reaction model being based on tracer diffusivity data of aluminium, silicon and oxygen

Peter Fielitz, Günter Borchardt, Martin Schmücker, Hartmut Schneider

A diffusion-controlled mullite formation reaction model being based on tracer diffusivity data of aluminium, silicon and oxygen

Journal:	*Philosophical Magazine & Philosophical Magazine Letters*
Manuscript ID:	TPHM-06-Feb-0031.R1
Journal Selection:	Philosophical Magazine
Date Submitted by the Author:	05-Jul-2006
Complete List of Authors:	Fielitz, Peter; Institut für Metallurgie, TU Clausthal Borchardt, Günter; Institut für Metallurgie, TU Clausthal Schmücker, Martin; Institut für Werkstoff-Forschung, Deutsches Zentrum für Luft- und Raumfahrt Schneider, Hartmut; Institut für Werkstoff-Forschung, Deutsches Zentrum für Luft- und Raumfahrt
Keywords:	ceramics, defects in solids, diffusion, high-temperature materials, SIMS
Keywords (user supplied):	mullite, tracer diffusion, formation reaction model

Philosophical Magazine, submitted, revised

A diffusion-controlled mullite formation reaction model being based on tracer diffusivity data of aluminium, silicon and oxygen

P. FIELITZ*†, G. BORCHARDT†, M. SCHMÜCKER‡ and H. SCHNEIDER‡

†Institut für Metallurgie, Technische Universität Clausthal,
D-38678 Clausthal-Zellerfeld, Germany

‡Institut für Werkstoff-Forschung, Deutsches Zentrum für Luft- und Raumfahrt,
D-51147 Köln, Germany

* corresponding author: e-mail: peter.fielitz@tu-clausthal.de
phone: +49/5323/72-2634
fax: +49/5323/72-3184

This paper compiles all data of our tracer diffusivity studies in single crystalline 2/1-mullite. As tracers we used the rare stable isotopes ^{18}O and ^{30}Si and the artificial pseudo-stable isotope ^{26}Al. Secondary Ion Mass Spectrometry was applied to analyse the depth distribution of the tracer isotopes after the diffusion annealing. An essential result of our tracer diffusivity studies was the very low diffusivity of ^{30}Si compared to the diffusivities of ^{26}Al and ^{18}O, which are almost equal. Based on this observation we propose a reaction model for the diffusion-controlled mullite formation in the solid state, which assumes that the growth kinetics of a mullite layer is mainly controlled by the diffusion of aluminium ions and oxygen ions.

Keywords: mullite; tracer diffusion; formation reaction model

1. Introduction

Mullite is one of the most widely studied ceramic materials. This is due to its high thermal and chemical stability, good thermal shock behaviour and high creep resistance, which makes mullite a promising candidate for many high-temperature applications [1]. The crystal structure of mullite can be described as a modified defect structure of sillimanite ($Al_2O_3 \bullet SiO_2$). Sillimanite consists of edge-sharing aluminium-oxygen octahedral chains which are interconnected by double chains of ordered SiO_4 and AlO_4 tetrahedra. In mullite, the AlO_4-SiO_4-sequence is almost random [2] and there exists a certain amount of structural oxygen vacancies. The composition of mullite can be expressed as $Al_2^{VI}(Al_{2+2x}^{IV}Si_{2-2x})O_{10-x}$ where x indicates the amount of missing oxygen with respect to sillimanite and VI and IV indicate sixfold (octahedral) and fourfold (tetrahedral) coordination of aluminium ions. Silicon ions occupy tetrahedral sites only.

Sintering, grain growth, creep and all types of reconstructive reaction processes are strongly controlled by atomic diffusion. Therefore, the diffusivities of oxygen and silicon in single crystalline 2/1-mullite have been carefully determined in previous work using the rare natural isotopes ^{18}O and ^{30}Si as tracer isotopes [3], [4]. Secondary Ion Mass Spectrometry (SIMS) was applied to analyse the depth distribution of the tracer isotopes after the diffusion annealing. Recently, we applied the SIMS technique also to measure the diffusivity of aluminium in single crystalline 2/1-mullite using the pseudo-stable isotope ^{26}Al [5] so that we can now present a complete set of tracer diffusivity data (^{18}O, ^{30}Si, ^{26}Al) of all components of the mullite structure. Based on the results of these tracer diffusivity studies a reaction model for the diffusion controlled mullite formation is discussed in the following.

2. Experimental data

For all tracer diffusion experiments single crystalline 2/1 mullite disks (≈ 1 mm thick) cut perpendicular to [010] and [001] were used to measure the tracer diffusivities along the crystallographic b and c axes. The single crystals were synthesized by Dr. W. Walraffen (Univ. Bonn, Germany) using the Czochralski technique. Details of the crystal growth procedure were published by Guse and Mateika [6].

The b and c axes are very different from a crystallographic point of view, because the mullite structure consists of chains of edge-sharing AlO_6 octahedra running parallel to the crystallographic c axis. These AlO_6 chains are cross-linked by (Al, Si)O_4 tetrahedra forming double chains, which also run parallel to c [1]. Therefore, a pronounced anisotropy of the diffusivities of the constituents could not be excluded a priori. However, all experimental tracer diffusivity data display virtually no orientation-dependent variation. The slight difference between b and c axes falls into the estimated error range of ± 30 % of diffusion data gained by the method of SIMS depth profiling. Therefore, all evaluated Arrhenius relations represent average values deduced from the diffusivity measurements along the two axes. Since structural arrangements along the a and b axes are very similar in mullite, tracer diffusivities parallel to both directions should also be in a comparable range. So it may be justified to consider tracer diffusivities of the components to be isotropic in mullite.

- Oxygen tracer diffusion

Oxygen diffusion is well studied in many oxides because it can be measured relatively simply by gas/solid exchange experiments [7]. We performed ^{18}O isotope exchange experiments on single crystalline 2/1-mullite samples [3] and obtained the following Arrhenius relation:

$$D_{18O}^{2/1} = (3.71\,^{+13}_{-3}) \times 10^{-5}\,\frac{m^2}{s}\,\exp\left(-\frac{(433 \pm 21)\,kJ/mol}{RT}\right) \quad (1)$$

In 3/2-mullite, Ikuma et al. [8] evaluated the ^{18}O tracer diffusivity indirectly on micrometer size single crystals by measuring the concentration of $^{18}O_2$ in the gas phase:

$$D_{18O}^{3/2} = (1.32 \pm 0.39) \times 10^{-6}\,\frac{m^2}{s}\,\exp\left(-\frac{(397 \pm 45)\,kJ/mol}{RT}\right) \quad (2)$$

- Silicon tracer diffusion

In contrast to oxygen, the measurement of silicon diffusivities in oxides is much more difficult. The complications arise from the fact that the natural tracer isotope ^{30}Si has a relatively high natural abundance of about 3.1 %. This circumstance limits the useful diffusion length and requires a deposition technique that allows to prepare very smooth ^{30}Si containing layers on the surface of the specimen. A detailed description of the experimental procedure is given in [4]. The following Arrhenius relation was obtained for the diffusivity of ^{30}Si in single crystalline 2/1-mullite:

$$D_{30Si}^{2/1} = (7.3\,^{+108}_{-6.8}) \times 10^{-2}\,\frac{m^2}{s}\exp\left(-\frac{(612 \pm 39)kJ/mol}{RT}\right) \quad (3)$$

- Aluminium tracer diffusion

Aluminium has no natural tracer isotopes and there are only a few aluminium diffusion data in the literature measured by means of the radiotracer isotope ^{26}Al [9]-[13]. The reason is that two difficulties are encountered with this radiotracer. Firstly, ^{26}Al is artificial and causes very high production costs, and secondly, it has a half-life time of 7.4×10^5 years with a very low specific activity which makes it difficult to apply classical radiotracer methods [12]. The application of SIMS avoids the problems related to the radioactivity measurement, reduces the necessary amount of ^{26}Al per experiment considerably, and yields a much higher spatial resolution. A detailed description of the measurement of the ^{26}Al diffusivity in 2/1- mullite by means of the SIMS technique is given in [5]. For the diffusivity of ^{26}Al in single crystalline 2/1-mullite we obtained the following Arrhenius relation:

$$D_{26Al}^{2/1} = (9.2\,^{+92}_{-8.4}) \times 10^{-3}\,\frac{m^2}{s}\exp\left(-\frac{(517 \pm 33)kJ/mol}{RT}\right) \quad (4)$$

[*Insert Fig. 1 about here*]

Fig. 1 shows our measured tracer diffusivities (^{18}O, ^{26}Al, ^{30}Si) in single crystalline 2/1-mullite and the ^{18}O diffusivity in single crystalline 3/2-mullite measured by Ikuma et al. [8]. There is only a small difference between the ^{18}O diffusivity in 2/1-mullite and 3/2-mullite. One observes that the diffusivity of ^{30}Si is much lower than the diffusivity of ^{18}O and ^{26}Al. Jaoul et al. [14] and Andersson et al. [15] measured ^{30}Si diffusivities in single crystalline forsterite Mg_2SiO_4 along three crystallographic directions. Both observed that in this silicate, too, silicon diffuses more slowly than oxygen and found no significant anisotropy of the diffusion coefficients. It is assumed that the strong covalent bond within the SiO_4 tetrahedron is an explanation for the low diffusivity of silicon. Furthermore, one observes from Fig. 1 that the diffusivity of ^{26}Al is comparable to the diffusivity of ^{18}O. Le Gall et al. [12] reported a similar result for the diffusivities of ^{26}Al and ^{18}O in single crystalline α-Al_2O_3.

The solid points in Fig. 1 at higher temperatures are experimental data of the parabolic growth

constant, k, of diffusion-controlled mullite formation, intensively investigated by Aksay et. al [16], [17]. The quoted authors used diffusion couples made from sapphire and aluminium-silicate glasses of 10.9, 22.8, and 42.2 wt % Al_2O_3. These binary glasses are in equilibrium with mullite at 1678°C, 1753°C, and 1813°C. Thus, sapphire-glass diffusion couples of these compositions at the corresponding annealing temperatures could be used to study the growth kinetics of mullite as an intermediate phase without solution of mullite in the liquid glass phase. The thickness of the mullite layer increased linearly with the square root of time, indicating that the growth mechanism is diffusion-controlled. The results of Aksay's experiments are outlined in Table 1.

[*Insert Table 1 about here*]

The dashed lines in Fig. 1 are extrapolated tracer diffusivity data from lower temperatures. This means, we know the tracer diffusivities of all components of mullite and the question arises how the measured parabolic growth constants are related to our measured tracer diffusivities. To answer this interesting question we will propose a reaction model for the diffusion-controlled mullite formation in the next chapter.

3. Reaction model

Sung [18] proposed a diffusion-controlled reaction model which is based on the assumption that the oxygen mobility is much lower than the mobility of the cations in mullite. Our tracer diffusion experiments show, however, that silicon is the slowest species compared to oxygen and aluminium in single crystalline 2/1-mullite. This is most probably also valid for 3/2-mullite (s. [8] for the diffusivity of ^{18}O in 3/2-mullite, which is virtually identical to the oxygen diffusivity in 2/1-mullite, as shown in Fig. 1). We will use our experimental observation to derive a more realistic reaction model which is schematically represented in Fig. 2.

[*Insert Fig. 2 about here*]

Because of the low silicon tracer diffusivity we neglect Si^{4+} ion fluxes and consider a formation mechanism where Al_2O_3 is transported by Al^{3+} and O^{2-} ion fluxes through the mullite layer. The fluxes are described by a coordinate system which is fixed to the phase boundary I. Such a coordinate system becomes applicable when one cation has a much lower mobility than other species [19]. The intrinsic drift velocity, $d\xi/dt$, describes the drift velocity of phase boundary II relative to phase boundary I. A simple, but fundamental, relation between the Al^{3+} and O^{2-} fluxes in Fig. 2 is given in the absence of space charges

$$3\,j_{Al^{3+}} - 2\,j_{O^{2-}} = 0 \tag{5}$$

In the literature (p. 229 in [20]) one finds the concept of a molecular flux, $j_{A_\alpha B_\beta}$, and a molecular diffusion coefficient, $D_{A_\alpha B_\beta}$, which is used to express the fact that the process takes places as if an entity $A_\alpha B_\beta$ of fixed composition (a "molecule" or better a "formula unit") were migrating. The condition for a molecular flux of Al_2O_3 is

$$j_{Al_2O_3} = \frac{j_{Al^{3+}}}{2} = \frac{j_{O^{2-}}}{3} \tag{6}$$

where j_i is the flux of the ion i (Al^{3+}, O^{2-}). Equation (6) ensures the composition to remain constant and is identical to equation (5) which excludes any build-up of space charge. That is, one can describe the two coupled Al^{3+} and O^{2-} ion fluxes by a single molecular flux of Al_2O_3

$$j_{Al_2O_3} = -\frac{c_{Al_2O_3} D_{Al_2O_3}}{RT} \frac{d\mu_{Al_2O_3}}{dx} \tag{7}$$

were c is the molecular concentration, D the molecular (ambipolar) diffusion coefficient and μ the molecular chemical potential of Al_2O_3 in the solid mullite layer. In ceramics the term ambipolar diffusion coefficient is preferred as it implies the fact of the migration of coupled charges (p. 232 in [20] or p. 238 in [21]). For the ambipolar diffusion coefficient of Al_2O_3 in equation (7) one gets after a lengthy calculation (see appendix A.1)

$$\frac{1}{D_{Al_2O_3}} = \frac{2}{D_{Al^{3+}}} + \frac{3}{D_{O^{2-}}} \tag{8}$$

where D_i is the diffusion coefficient of the ion i (Al^{3+}, O^{2-}) which is related to the random thermal motion of the ions. In diffusional transport the random thermal motion is superposed on a drift resulting from field forces like the gradient of the chemical potential. Using equation (7) one gets for the average drift velocity of Al_2O_3

Comment [PF1]: In [19] siehe Note 2 auf S. 232 und Appendix IV auf S. 244. In [20] siehe Fußnote auf S. 238.

Comment [PF2]: Erläuterungen übernommen aus [21] S. 107.

$$v_{Al_2O_3} = \frac{j_{Al_2O_3}}{c_{Al_2O_3}} = -\frac{D_{Al_2O_3}}{RT}\frac{d\mu_{Al_2O_3}}{dx} \tag{9}$$

Since the forces ($d\mu_{Al_2O_3}/dx = 2\,d\mu_{Al^{3+}}/dx + 3\,d\mu_{O^{2-}}/dx$) are small on the atomic length scale, diffusion coefficients established under equilibrium conditions (i.e., vanishing forces) can be used to describe the drift of the ions (p. 107 in [22]).

The relation of the self diffusion coefficients, D_i, of the ions in equation (8) to our measured tracer diffusivities, D_{*_i}, is given by $D_{*_i} = f_{*_i} D_i$, where f_{*_i} is the so-called correlation factor (p. 97 in [20]). Correlation factors for self diffusion are calculated for different diffusion mechanisms and crystal structures and are often in the order of 1 (p. 98 in [20]). Therefore, we can calculate the ambipolar diffusion coefficient of Al_2O_3 in a first order approximation by our measured tracer diffusivities

$$\frac{1}{D_{Al_2O_3}} = \frac{2\,f_{^{26}Al}}{D_{^{26}Al}} + \frac{3\,f_{^{18}O}}{D_{^{18}O}} \cong \frac{2}{D_{^{26}Al}} + \frac{3}{D_{^{18}O}} \tag{10}$$

Correlation effects diminish the effectiveness of atomic jumps ($f_{*_i} \le 1$) in diffusional random motion (p. 110 in [22]), that is, ambipolar diffusion coefficients calculated by our tracer diffusivities are lower limits.

To calculate the parabolic growth constant, k, it is assumed that the ion fluxes are quasi-steady which means that during a specific time interval the fluxes can be considered to be constant in space. Because the concentration of Al_2O_3 is practically constant inside the mullite layer the drift velocity of Al_2O_3 is also practically independent of x. Separating variables and integrating equation (9) between the phase boundaries I and II results in (p. 168 in [22])

$$v_{Al_2O_3}\xi = -\frac{1}{RT}\int_{(I)}^{(II)} D_{Al_2O_3}\,d\mu_{Al_2O_3} \tag{11}$$

where ξ is the thickness of the mullite layer. The drift velocity of phase boundary II relative to phase boundary I is equal to the average drift velocity of the Al_2O_3 molecules, $d\xi/dt = v_{Al_2O_3}$, so that one calculates the parabolic growth constant, k, by separating variables and integrating equation (11)

$$k = \frac{\xi^2}{2t} = -\frac{1}{RT}\int_{(I)}^{(II)} D_{Al_2O_3}\,d\mu_{Al_2O_3} \tag{12}$$

To integrate the right hand side of equation (12) we must know the dependence of the ambipolar diffusion coefficient on the chemical potential which requires the application of an appropriate defect model.

Aksay et al. [17] used diffusion couples with sapphire and aluminium-silicate glasses at different temperatures. For every temperature, the Al_2O_3 concentration of the binary glass was chosen so that the glass phase was in equilibrium with the mullite phase. That is, any growth of the mullite layer requires Al_2O_3 to be transported through the mullite layer from the sapphire sample side. This transport is enabled by a flux of freely migrating defects which are formed during the mullite formation reaction. We assume that during the reaction of "SiO_2" from the binary glass with "Al_2O_3", which is located on regular sites in the mullite structure, aluminium vacancies and oxygen vacancies are formed according to the following reaction (applying the Kröger-Vink notation)

$$2\,SiO_2 + 6\,Al_{Al}^{\times} + 9\,O_O^{\times} = 6\,V_{Al}''' + 9\,V_O^{\bullet\bullet} + Al_6Si_2O_{13} \qquad (13)$$

where $Al_6Si_2O_{13}$ is 3/2-mullite. If local defect equilibrium is assumed one gets from equation (13) the defect equilibrium constant

$$K_d = \frac{a_{V_{Al}'''}^{6}\, a_{V_O^{\bullet\bullet}}^{9}}{a_{SiO_2}^{2}} \qquad (14)$$

where a_i is the activity of the species i (SiO_2, aluminium vacancies, oxygen vacancies). Furthermore, we assume that the dilution of the vacancies is sufficient to express activities by concentrations, $a_V \cong [V]$. Using the condition for electroneutrality, $3[V_{Al}'''] = 2[V_O^{\bullet\bullet}]$, one gets from equation (14) a dependence of the vacancy concentration from the SiO_2 activity

$$[V_{Al}'''] = \alpha\, a_{SiO_2}^{2/15} \quad \text{and} \quad [V_O^{\bullet\bullet}] = \frac{3}{2}\alpha\, a_{SiO_2}^{2/15} \quad \text{with} \quad \alpha \equiv \left(\frac{2}{3}\right)^{-3/5} K_d^{1/15} \qquad (15)$$

If the diffusivity of aluminium ions is proportional to the concentration of aluminium vacancies, $D_{Al^{3+}} \propto [V_{Al}''']$, and if the diffusivity of oxygen ions is proportional to the concentration of oxygen vacancies, $D_{O^{2-}} \propto [V_O^{\bullet\bullet}]$, one can conclude from equations (8) and (15) that the ambipolar diffusion coefficient of Al_2O_3 is proportional to $a_{SiO_2}^{2/15}$

$$D_{Al_2O_3} = D^{I}_{Al_2O_3}\left(\frac{a_{SiO_2}}{{}^{I}a_{SiO_2}}\right)^{2/15} \tag{16}$$

where the superscript I denotes values at the phase boundary I. Inserting equation (16) into equation (12) gives after some calculations (see appendix A.2)

$$k = n\,(D^{II}_{Al_2O_3} - D^{I}_{Al_2O_3}) \quad \text{with} \quad n = 5 \tag{17}$$

where the superscripts I and II denote values of the ambipolar diffusion coefficient at the corresponding phase boundaries in Fig. 2.

4. Discussion

The calculations in chapter 3 show that the parabolic growth constant, k, is proportional to the difference of the ambipolar diffusion coefficients of Al_2O_3 at the phase boundaries (see equation (17)) where the calculated proportional constant, n, depends on the applied defect model and is 5 for the proposed one (equation (13)). It is interesting to note that only the difference of the absolute values of the ambipolar diffusion coefficients plays a role for the diffusion controlled growth kinetics of the reaction layer (mullite). The absolute values of the ambipolar diffusion coefficients of Al_2O_3 at both phase boundaries are determined by the freely migrating defects which are formed during the mullite formation reaction. Equation (17) would be the most direct way to calculate parabolic growth constants from diffusivity data. However, this procedure requires the same defect chemistry to be valid for the entire composition range of mullite and it requires the measurements of the two diffusion constants.

Because diffusivity measurements are often only possible at one of the two interfaces it is useful to express equation (17) by

$$k = D^{I}_{Al_2O_3}\Delta R \tag{18}$$

with the dimensionless factor

$$\Delta R = n\,\frac{D^{II}_{Al_2O_3} - D^{I}_{Al_2O_3}}{D^{I}_{Al_2O_3}} \tag{19}$$

where we have assumed that the ambipolar diffusion coefficient of Al_2O_3 at phase boundary I corresponds to our calculated ambipolar diffusion coefficient of Al_2O_3 from the measured

tracer diffusivity data. The disadvantage of this notation is that it seems to suggest that $D^{I}_{Al_2O_3}$ and the dimensionless factor, ΔR, are independent terms, with the wrong implication that k is proportional to the absolute value of $D^{I}_{Al_2O_3}$. The advantage of this notation will, however, become obvious in the development given below.

The diffusivities at the interfaces are proportional to the freely migrating defects at the interfaces so that one gets for the dimensionless factor ΔR (considering equations (15) and (16))

$$\Delta R = n\frac{[V'''_{Al}]^{II} - [V'''_{Al}]^{I}}{[V'''_{Al}]^{I}} = n\frac{[V^{\bullet\bullet}_{O}]^{II} - [V^{\bullet\bullet}_{O}]^{I}}{[V^{\bullet\bullet}_{O}]^{I}} \tag{20}$$

As ΔR is proportional to the relative change of the concentrations of the transporting defects it can be calculated from our proposed defect model (see appendix A.3)

$$\Delta R = 5\left[(a^{II}_{SiO_2})^{\frac{2}{15}}\exp\left(-\frac{\Delta_r G^{\circ}_{Al_6Si_2O_{13}}}{15RT}\right) - 1\right] \tag{21}$$

where $\Delta_r G^{\circ}_{Al_6Si_2O_{13}}$ is the Gibbs free energy for the formation of 3/2-mullite from the parent oxides and $a^{II}_{SiO_2}$ is the activity of SiO_2 in the aluminium-silicate melt at phase boundary II.

In the absence of any plausible defect model one could assume, as a first approximation, a constant diffusion coefficient, $D_{Al_2O_3} = D^{I}_{Al_2O_3} = D^{II}_{Al_2O_3}$, which allows the simplest integration of the right hand side of equation (12). This gives

$$k_0 = D^{I}_{Al_2O_3}\,\Delta R_0 \tag{22}$$

with the dimensionless factor ΔR_0

$$\Delta R_0 = \frac{\left|\Delta\mu_{Al_2O_3}\right|}{RT} \quad \text{and} \quad \Delta\mu_{Al_2O_3} = \mu^{II}_{Al_2O_3} - \mu^{I}_{Al_2O_3} \tag{23}$$

where the superscripts I and II denote values of the chemical potential of Al_2O_3 at the corresponding phase boundaries in Fig. 2 and the subscript 0 indicates values of a first approximation. The difference of the chemical potential of Al_2O_3 at both phase boundaries can be calculated by means of the Gibbs free energy of formation of 3/2-mullite from the oxides and the activity of SiO_2 in the aluminium-silicate melt at phase boundary II (see appendix A.4).

$$\Delta\mu_{Al_2O_3} = \frac{\Delta_r G^{\circ}_{Al_6Si_2O_{13}}}{3} - \frac{2}{3} RT \ln(a^{II}_{SiO_2}) \quad (24)$$

[*Insert Table 2 about here*]

The dimensionless factors ΔR_0 and ΔR for the 3/2-mullite formation from the oxides are calculated in Table 2 for experimental temperatures used by Aksay et. al [17] (see Table 1). It is obvious that both factors are practically equal in this temperature range. Comparing equations (18) and (22) through the ratio

$$\frac{k}{k_0} = \frac{\Delta R}{\Delta R_0} = \frac{5\left[\left(a^{(II)}_{SiO_2}\right)^{\frac{2}{15}} \exp\left(-\frac{\Delta_r G^{\circ}_{Al_6Si_2O_{13}}}{15RT}\right) - 1\right]}{-\frac{\Delta_r G^{\circ}_{Al_6Si_2O_{13}}}{3RT} + \frac{2}{3}\ln(a^{(II)}_{SiO_2})} \quad (25)$$

one can conclude that the reason for this observation is the low value of the Gibbs free energy, $\Delta_r G^{\circ}_{Al_6Si_2O_{13}} \approx -35\,kJ/mol$, for the formation of 3/2-mullite from the oxides and the high experimental temperatures, $RT \approx 17\,kJ/mol$. Therefore, our proposed defect model does practically not improve the agreement between the experimental data and the calculated parabolic growth rates in this temperature range, so that it is not meaningful to try a quantitatively validation of this model. It is, however, extremely useful to discuss this phenomenon from a more general point of view. The derivation of the factor of first approximation, ΔR_0, starts with the assumption that the (chemical) diffusion coefficient, D, in the reaction layer is practically constant and we assume, of course, that the calculated parabolic growth rate is practically correct, which implies the approximate relation

$$\frac{\Delta R_0}{n} \approx \frac{\Delta R}{n} \quad \text{if} \quad D \approx \text{constant} \quad (26)$$

where n is a correct number evaluated from a correct defect model. Considering equations (23) and (19) we can express relation (26) by

$$\left|\frac{\Delta\mu_i}{nRT}\right| \approx \left|\frac{D_i^{II} - D_i^{I}}{D_i^{I}}\right| \quad \text{if} \quad D \approx \text{constant} \quad (27)$$

where $i = Al_2O_3$ for the proposed mullite formation reaction. Such a relation holds for all

formation reactions which can be treated mathematically in the same formal manner.

The right hand side of relation (27) corresponds to the relative change of the diffusivity across the mullite layer. That is, the assumption that the diffusion coefficient in the reaction layer is practically constant is fulfilled if $|\Delta\mu_i| < |n|RT$. This case is generally more likely at higher temperatures and reactions with low Gibbs free energy of formation (e.g the considered mullite formation from the oxides). One has then $\Delta R_0 \approx \Delta R$ and can calculate the parabolic growth constant by the simple equation (22). The application of a defect model does practically not improve the calculated parabolic growth constants in the considered temperature range so that it becomes difficult to prove a proposed defect model quantitatively from experimentally determined parabolic growth constants.

The case $|\Delta\mu_i| > |n|RT$ is clearly in conflict with relation (27) which is based on the assumption that the diffusion coefficient in the reaction layer is approximately constant. This case is generally more likely at lower temperatures and reactions with high Gibbs free energy of formation. It is then not reasonable to assume a constant diffusion coefficient to integrate equation (12), so that an appropriate defect model is necessary to calculate parabolic growth constants.

The measured parabolic growth rates of 3/2-mullite are by a factor of 4 to 17 larger (see the ratio k_{exp}/k_{calc} in Table 2) than the parabolic growth rates calculated from our measured tracer diffusivities in single crystalline 2/1-mullite. Two terms were used to calculate the theoretical parabolic growth rates (see equation (18)): a diffusivity term and a dimensionless term, the factor, ΔR, which could be expressed in a good approximation by the normalised change of the chemical potential of Al_2O_3, $|\Delta\mu_{Al_2O_3}|/RT$, across the reaction layer. Hence, a strong deviation from the experimental values cannot be explained by a wrong calculation of the factor, ΔR, because this would imply a very erroneous calculation of the chemical potential of Al_2O_3. The observed deviation from the experimental values must be induced by the calculation of the diffusivity term in equation (18). This term was calculated by equation (10) using our measured bulk tracer diffusivities. As we mentioned above the use of tracer diffusivities, and neglecting correlation effects, will result principally in a lower limit value of the diffusivity term in equation (18). Furthermore, grain boundary diffusion has to be considered to explain why the diffusivities of the oxygen ions and the aluminium ions during

the mullite formation are significantly higher than our measured bulk tracer diffusivities.

Grain boundary tracer diffusivities of mullite are known for the ^{18}O isotope only [23]. In the grain boundaries a much higher ^{18}O diffusivity (up to a factor of 10^4) was observed than in the bulk. The amount of Al_2O_3 which is transported through the grain boundaries is proportional to the volume fraction of grain boundaries in the mullite layer. Therefore, an effective diffusion coefficient can be calculated by the Hart-Mortlock equation [24][25]

$$D_{eff} = s\,g\,D_{gb} + (1 - s\,g)\,D \qquad (28)$$

where D is the bulk diffusivity, D_{gb} the grain boundary diffusivity, g the volume fraction of grain boundaries, and s the grain boundary segregation factor ($s = 1$ for self-diffusion). Assuming a similar enhancement (a factor of 10^4) of the ^{26}Al diffusivities in the grain boundaries one can conclude from the Hart-Mortlock equation that volume fractions of grain boundaries from 2.9×10^{-4} to 1.6×10^{-3} are sufficient to explain the observed discrepancies between calculated and measured parabolic growth rates. For a cubic grain geometry one can estimate the grain size, d, by $d \approx 3\delta / g$ (p. 206 in [26]). Assuming an average grain boundary width $\delta = 1$ nm one gets corresponding cubic grain sizes from 10 µm to 2 µm.

This explanation is plausible, however, the larger discrepancy at higher temperatures is somewhat contradictory to conventional thinking about grain boundary effects (i.e., the relative contribution from grain boundary diffusion is often larger at lower temperatures). Another explanation could be impurity effects on diffusion, even with relatively pure starting materials. For example, one observes a scatter band of about one order of magnitude for measured oxygen diffusivities in nominally undoped α-Al_2O_3 which is mainly explained by impurities which induce extrinsic point defects and affect the diffusion process [27]. Furthermore, we have assumed that the influence of the Si/Al ratio does not strongly affect the diffusion process. This assumption is based on the low value of the Gibbs free energy of formation of mullite and on the resulting close agreement of the oxygen diffusivity data obtained for (single crystalline) 2/1-mullite and 3/2-mullite (see also [28] for further discussion) but is open to debate for the aluminium diffusivity.

This discussion shows that the parabolic growth rates calculated from our measured bulk tracer diffusivity data of oxygen and aluminium define at least a lower limit of the experimentally observed growth rates. With the exception of the mullite formation data set at the highest temperature (1813 °C) the discrepancy between parabolic rate constants calculated

on the basis of (extrapolated) bulk diffusion data and the experimentally determined rate constants is about half an order of magnitude, which clearly supports our model, taking into account that the details of the growth experiment (impurity concentrations etc.) are not fully evident from the literature.

5. Summary

An essential result of our tracer diffusivity studies in single crystalline 2/1-mullite is the very low diffusivity of ^{30}Si compared to the diffusivities of ^{26}Al and ^{18}O, which are almost equal. Based on this observation we propose a diffusion-controlled mullite formation model which assumes that the growth kinetics of a mullite layer is controlled by the diffusion of aluminium ions and oxygen ions. The two ionic fluxes can be described by a single molecular (ambipolar) flux of Al_2O_3 which transports Al_2O_3 through the mullite layer and reacts with SiO_2 to mullite. The ambipolar flux of Al_2O_3 is enabled by freely migrating defects which are formed during the mullite formation reaction.

The reaction of SiO_2 with Al_2O_3 on regular sites in the mullite structure requires the formation of aluminium vacancies and oxygen vacancies (equation (13)). Based on this defect model we derive equation (17) to calculate the parabolic growth constant of mullite formation. However, the direct application of this equation requires the proposed defect model to be valid in the whole mullite layer and necessitates the measurement of tracer diffusivities at the two interfaces. Therefore, we write equation (17) into the form of equation (18) by the definition of a dimensionless factor, ΔR, and assume that the ambipolar diffusion coefficient of Al_2O_3 at interface I corresponds to the ambipolar diffusion coefficient of Al_2O_3 calculated from our tracer diffusivity data. The factor, ΔR, is then calculated by means of the proposed defect model (see equation (21)).

Further, it is demonstrated that because of the fairly low value of the Gibbs free energy of formation of mullite the ambipolar diffusion coefficient of Al_2O_3 in the mullite layer is practically constant.

To calculate the parabolic growth rate of mullite formation we need the ambipolar diffusion coefficient of Al_2O_3 in the mullite layer which can principally be calculated from the diffusion coefficients of aluminium and oxygen (equation (8)). Neglecting correlation effects we calculate the ambipolar diffusion coefficient of Al_2O_3 from our measured tracer diffusivity

data (equation (10)). The results of this calculation are compiled in Table 2 and show that our calculated values are about a factor of 5 lower than the measured values by Aksay et al. [17], at least below 1750 °C. Taking into account typical experimental errors in layer growth experiments this fairly small discrepancy supports our reaction model. Our calculated values thus define a lower limit of the parabolic growth rate.

Acknowledgement

Financial support from Deutsche Forschungsgemeinschaft (DFG) is gratefully acknowledged. The comments of an anonymous reviewer helped to improve the manuscript.

Appendix A

For the following derivations it is assumed that local thermodynamical equilibrium is maintained within the reaction layer and also at the phase boundaries I and II, so that the following equilibrium condition is valid

$$2\,Al^{3+} + 3\,O^{2-} = Al_2O_3 \tag{29}$$

$$2\,\eta_{Al^{3+}} + 3\,\eta_{O^{2-}} = \mu_{Al_2O_3} \tag{30}$$

where η is the electrochemical potential of electrically charged particles (Al^{3+}, O^{2-}) and μ is the chemical potential of the uncharged particle (Al_2O_3). The chemical reaction equation of the 3/2-mullite formation from the oxides is given by

$$2\,SiO_2 + 3\,Al_2O_3 = Al_6Si_2O_{13} \tag{31}$$

The reaction equilibrium constant, K_r, can be written as

$$K_r = \frac{a_{Al_6Si_2O_{13}}}{a^3_{Al_2O_3}\,a^2_{SiO_2}} = \exp\left(-\frac{\Delta_r G^\circ_{Al_6Si_2O_{13}}}{RT}\right) \tag{32}$$

where a_i is the activity of component i ($Al_6Si_2O_{13}$, Al_2O_3, SiO_2) and $\Delta_r G^\circ_{Al_6Si_2O_{13}}$ is the Gibbs free energy of formation of 3/2-mullite from the oxides which can be calculated by the free energy of the formation from elements, $\Delta_f G^\circ_i$ tabulated in [29] or [30],

$$\Delta_r G^\circ_{Al_6Si_2O_{13}} = \Delta_f G^\circ_{Al_6Si_2O_{13}} - 3\Delta_f G^\circ_{Al_2O_3} - 2\Delta_f G^\circ_{SiO_2} \tag{33}$$

The activity of 3/2-mullite is 1 in the mullite layer so that equation (32) yields

$$2\,RT\ln\left(a_{SiO_2}\right) + 3\,RT\ln\left(a_{Al_2O_3}\right) = \Delta_r G^\circ_{Al_6Si_2O_{13}} \tag{34}$$

A.1 Derivation of equation (8)

The fluxes of aluminium and oxygen ions are given by

$$j_{Al^{3+}} = -\frac{c_{Al^{3+}}\,D_{Al^{3+}}}{RT}\frac{d\eta_{Al^{3+}}}{dx} \tag{35}$$

$$j_{O^{2-}} = -\frac{c_{O^{2-}}\,D_{O^{2-}}}{RT}\frac{d\eta_{O^{2-}}}{dx}$$

where c_i, D_i and η_i are the concentration, the diffusion coefficient and the electrochemical potential of the ion i (Al^{3+}, O^{2-}), respectively [31]. The gradient of the electrochemical potentials can be expressed by

$$\frac{d\eta_{Al^{3+}}}{dx} = \frac{d\mu_{Al^{3+}}}{dx} + 3F\frac{d\varphi}{dx} \tag{36}$$

$$\frac{d\eta_{O^{2-}}}{dx} = \frac{d\mu_{O^{2-}}}{dx} - 2F\frac{d\varphi}{dx}$$

where F is the Faraday constant and φ the electrical potential. The condition for electroneutrality, equation (5), is used to eliminate the unknown term F×dφ/dx from the flux equations.

$$F\frac{d\varphi}{dx} = -\frac{3c_{Al^{3+}}D_{Al^{3+}}\frac{d\mu_{Al^{3+}}}{dx} - 2c_{O^{2-}}D_{O^{2-}}\frac{d\mu_{O^{2-}}}{dx}}{9c_{Al^{3+}}D_{Al^{3+}} + 4c_{O^{2-}}D_{O^{2-}}} \tag{37}$$

Inserting equation (37) into the flux equations (35)-(36) and respecting equation (5) and (30) one gets for the ion fluxes

$$\frac{j_{Al^{3+}}}{2} = \frac{j_{O^{2-}}}{3} = -\frac{\langle cD \rangle_{Al_2O_3}}{RT}\frac{d\mu_{Al_2O_3}}{dx} \tag{38}$$

with the shortcut

$$\langle cD \rangle_{Al_2O_3} \equiv \frac{c_{Al^{3+}} D_{Al^{3+}} \times c_{O^{2-}} D_{O^{2-}}}{9 c_{Al^{3+}} D_{Al^{3+}} + 4 c_{O^{2-}} D_{O^{2-}}} \tag{39}$$

By equation (7) an ambipolar diffusion coefficient was defined. Comparing equations (6), (7) and (38) one concludes that the ambipolar diffusion coefficient is given by

$$D_{Al_2O_3} = \frac{\langle cD \rangle_{Al_2O_3}}{c_{Al_2O_3}} = \frac{D_{Al^{3+}} D_{O^{2-}}}{9 (c_{Al_2O_3} / c_{O^{2-}}) D_{Al^{3+}} + 4 (c_{Al_2O_3} / c_{Al^{3+}}) D_{O^{2-}}} \tag{40}$$

and finally because of the concentration relations

$$c_{Al_2O_3} = \frac{c_{Al^{3+}}}{2} = \frac{c_{O^{2-}}}{3} \tag{41}$$

one derives equation (8). Considering equation (6) and equation (41) one concludes

$$v = \frac{j_{Al_2O_3}}{c_{Al_2O_3}} = \frac{j_{Al^{3+}}}{c_{Al^{3+}}} = \frac{j_{O^{2-}}}{c_{O^{2-}}} \tag{42}$$

Thus, all particles (Al_2O_3, Al^{3+}, O^{2-}) considered in the proposed mullite formation model migrate with the same drift velocity, v.

A.2 Derivation of equation (17)

By definition the chemical potential of Al_2O_3 is given by

$$\mu_{Al_2O_3} = \mu^{\circ}_{Al_2O_3} + RT \ln(a_{Al_2O_3}) \tag{43}$$

considering also equation (34) one can express equation (12) by

$$k = \frac{2}{3}\int_{(I)}^{(II)} D_{Al_2O_3}\, d\ln(a_{SiO_2}) = \frac{2}{3}\int_{(I)}^{(II)} \frac{D_{Al_2O_3}}{a_{SiO_2}}\, da_{SiO_2} \tag{44}$$

Inserting equation (16) gives

$$k = 5\frac{D^{I}_{Al_2O_3}}{(a^{I}_{SiO_2})^{2/15}}\left[(a^{II}_{SiO_2})^{2/15} - (a^{I}_{SiO_2})^{2/15}\right] = 5(D^{II}_{Al_2O_3} - D^{I}_{Al_2O_3}) \tag{45}$$

A.3 Derivation of equation (21)

The factor ΔR is defined by equation (18). Considering equations (45) and (16) gives

$$\Delta R = 5\left[\frac{(a^{II}_{SiO_2})^{2/15}}{(a^{I}_{SiO_2})^{2/15}} - 1\right] \tag{46}$$

At interface I the activity of Al_2O_3 is 1 (see Fig. 2) so that one can calculate the activity of SiO_2 at interface I using equation (34)

$$(a^{I}_{SiO_2})^{2/15} = \exp\left(\frac{\Delta G^{\circ}_{Al_6Si_2O_{13}}}{15\,RT}\right) \tag{47}$$

Inserting equation (47) into equation (46) gives equation (21).

A.4 Derivation of equation (24)

The activity of Al_2O_3 is 1 at interface I and $a^{II}_{Al_2O_3}$ at interface II (see Fig. 2) so that one gets from equation (43) for the difference of the chemical potential

$$\Delta\mu_{Al_2O_3} = \mu^{II}_{Al_2O_3} - \mu^{I}_{Al_2O_3} = RT\ln(a^{II}_{Al_2O_3}) \tag{48}$$

Considering equation (34) one gets equation (24).

References

[1] H. Schneider, K. Okada and J.A. Pask, *Mullite and Mullite Ceramics* (John Wiley & Sons Ltd., Chichester, 1994).

[2] M. Schmücker, K.J.D. MacKenzie, M.E. Smith, D.L. Carroll and H. Schneider, J. Am. Ceram. Soc. **88** 2935 (2005).

[3] P. Fielitz, G. Borchardt, M. Schmücker, H. Schneider, M. Wiedenbeck, D. Rhede, S. Weber and S. Scherrer, J. Am. Ceram. Soc. **84** [12] 2845 (2001).

[4] P. Fielitz, G. Borchardt, M. Schmücker and H. Schneider, Phys. Chem. Chem. Phys. **5** 2279 (2003).

[5] P. Fielitz, G. Borchardt, M. Schmücker and H. Schneider, Solid State Ionics (2006), in press.

[6] W. Guse and D. Mateika, J. Cryst. Growth **22** 237 (1974).

[7] P. Fielitz and G. Borchardt, Solid State Ionics **144** 71 (2001).

[8] Y. Ikuma, E. Shimada, S. Sakano, M. Oishi, M. Yokoyama and Z. Nakagawa, J. Electrochem. Soc. **146** 4672 (1999).

[9] A.E. Paladino and W.D. Kingery, J. Chem. Phys. **37** 957 (1962).

[10] M. Beyeler and Y. Adda, J. Physique **29** 345 (1968).

[11] L.N. Larikov, V.V. Geichenko and V.M. Fal'chenko, *Diffusion Processes in Ordered Alloys* (Amerind Publ. Co, New Delhi, 1981) pp. 111–121.

[12] M. Le Gall, B. Lesage and J. Bernardini, Phil. Mag. A **70** 761 (1994).

[13] G.H. Frischat, J. Am. Ceram. Soc. **52** 625 (1969).

[14] O. Jaoul, M. Poumellec, C. Froidevaux and A. Havette, in *Anelasticity in the Earth*, edited by F.D. Stacey et al. (Geodyn. Ser. Vol. 4, AGU, Washington, DC, 1981) pp. 95–100.

[15] K. Andersson, G. Borchardt, S. Scherrer and S. Weber, Fresenius Z. Anal. Chem. **333** 383 (1989).

[16] I.A. Aksay, Diffusion and Phase Relationship Studies in the Alumina-Silica System. PhD thesis, University of California, Berkeley (1973).

[17] I.A. Aksay and J.A. Pask, J. Am. Ceram. Soc. **58** [11-12] 507 (1975).

[18] Y.-M. Sung, Acta mater. **48** 2157 (2000).

[19] A.R. Cooper Jr. and J.H. Heasley, J. Am. Ceram. Soc. **49** [5] 280 (1966).

[20] J. Philibert, *Atom Movements - Diffusion and Mass Transport in Solids* (Les Éditions de Physique, Les Ulis Cedex A, 1991).

[21] Y.-M. Chiang, D.P. Birnie and W.D. Kingery, *Physical Ceramics: Principles for Ceramic Science and Engineering* (John Wiley & Sons, New York, 1997).

[22] H. Schmalzried, *Chemical Kinetics of Solids* (VCH, Weinheim, 1995).

[23] P. Fielitz, G. Borchardt, M. Schmücker, H. Schneider and P. Willich, J. Am. Ceram. Soc. **87** [12] 2232 (2004).

[24] E.W. Hart, Acta Metall. **5** 597 (1957).

[25] A.J. Mortlock, Acta Metall. **8** 132 (1960).

[26] I. Kaur, Y. Mishin, W. Gust, *Fundamentals of Grain and Interphase Boundary Diffusion* (John Wiley & Sons Ltd., Chichester, 1995).

[27] D. Prot and C. Monty, Phil. Mag. A **73** [4] 899 (1996).

[28] P. Fielitz, G. Borchardt, M. Schmücker and H. Schneider, J. Eur. Ceram. Soc. **21** 2577 (2001).

[29] I. Barin, *Thermochemical Data of Pure Substances* (Part I + II, VCH Publishers, Weinheim, 1989).

[30] M.W. Chase Jr., C.A. Davies, J.R. Downey Jr., D.J. Frurip, R.A. McDonald and A.N. Syverud, *JANAF Thermochemical Tables* (3rd ed., ACS, AIP, NBS, New York, 1986).

[31] H. Schmalzried, *Solid State Reactions* (2^{nd} ed., Verlag Chemie, Weinheim, 1981).

Tables

Table 1 Experimental conditions and data for sapphire-equilibrium-melt runs [17], where t is the annealing time, ξ is the mullite layer thickness, and k_{exp} the experimental parabolic growth constant.

T °C	Melt mol % Al_2O_3	Mullite mol % Al_2O_3	t min	ξ µm	$k_{exp} = \xi^2/(2t)$ m^2/s
1678	6.75	58.6-62.7	12,182	10	6.8×10^{-17}
1678	6.75	58.6-62.7	47,380	18	5.7×10^{-17}
1753	14.9	58.6-62.7	6,608	13	2.1×10^{-16}
1813	30.2	59.9-62.7	10,025	36	1.1×10^{-15}

Table 2 Parabolic growth rates calculated from the measured tracer diffusivities of aluminium and oxygen using equations (10), (18) and (21) (compare with experimental data in Table 1). The activity of SiO_2 at phase boundary II, $a^{II}_{SiO_2}$, was approximated by the molar fraction of SiO_2 in the aluminium-silicate melt. The free energy, $\Delta_r G^\circ_{Al_6Si_2O_{13}}$, for the formation of 3/2-mullite from the oxides was calculated with equation (33) using thermochemical data from [29]. The dimensionless factor of first approximation, ΔR_0, was calculated by equations (23), (24).

T °C	RT kJ/mol	$\Delta_r G^\circ_{Al_6Si_2O_{13}}$ kJ/mol	$a^{II}_{SiO_2}$	ΔR_0	ΔR	$D_{Al_2O_3}$ m^2/s	k_{calc} m^2/s	k_{exp} / k_{calc}
1678	16.2	-33.8	0.93	0.65	0.69	2.1×10^{-17}	1.5×10^{-17}	4.6
1678	16.2	-33.8	0.93	0.65	0.69	2.1×10^{-17}	1.5×10^{-17}	3.9
1753	16.8	-35.3	0.85	0.59	0.63	6.1×10^{-17}	3.8×10^{-17}	5.6
1813	17.3	-36.5	0.70	0.46	0.48	1.3×10^{-16}	6.4×10^{-17}	17

Figure Captions

Fig. 1 Compilation of our measured tracer diffusivities (^{18}O, ^{26}Al, ^{30}Si) in single crystalline 2/1-mullite. Ikuma et al. [8] measured the ^{18}O diffusivity in single crystalline 3/2-mullite. Also shown are data of the parabolic growth constant, k, of mullite formation measured by Aksay et al. [17] via high-temperature diffusion couple experiments.

Fig. 2 Schematic representation of the reaction model for the mullite formation. Al_2O_3 is transported through the solid mullite layer by means of intrinsic Al^{3+} and O^{2-} ion fluxes and reacts to 3/2-mullite with SiO_2 from the aluminosilicate melt which is in equilibrium with mullite. The chemical potential of Al_2O_3 decreases across the mullite layer, the limiting values are $\mu^{I}_{Al_2O_3}$ in α-Al_2O_3 and $\mu^{II}_{Al_2O_3}$ in the aluminosilicate melt.

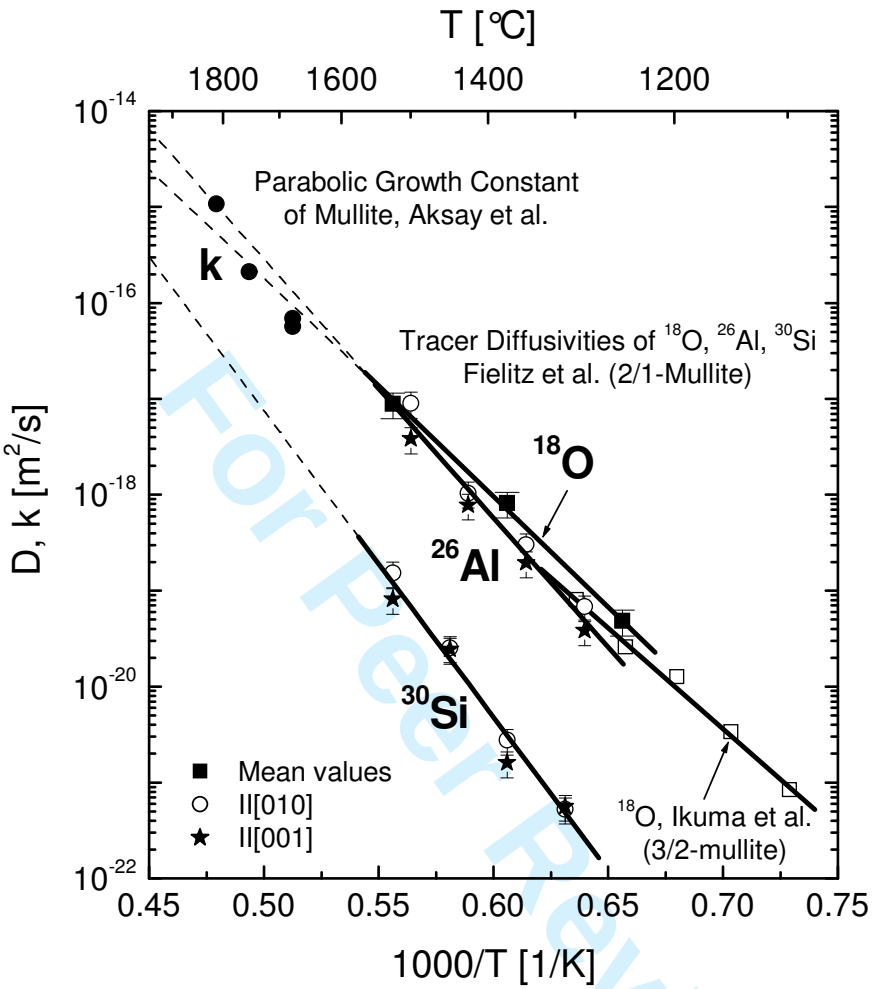

Fig. 1

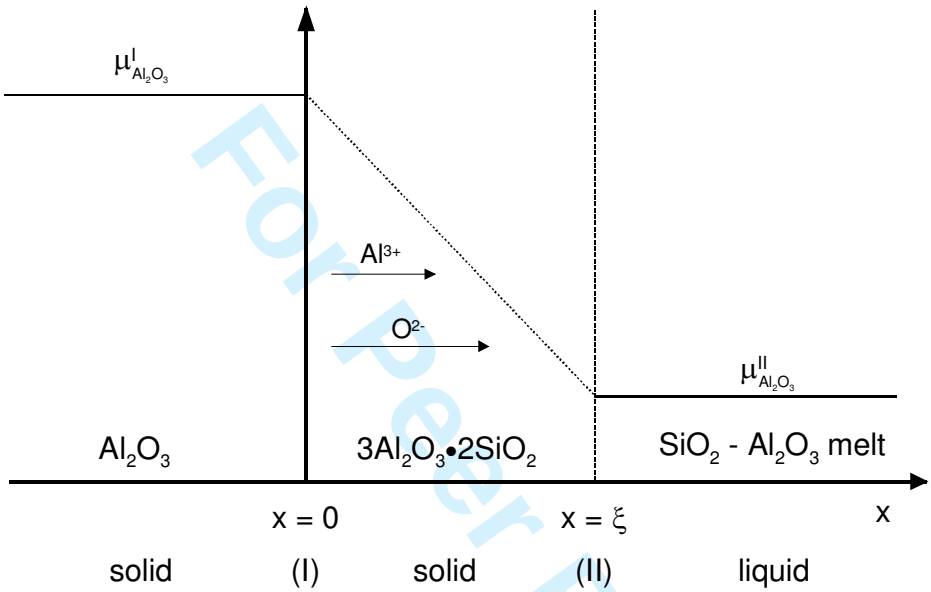

Fig. 2

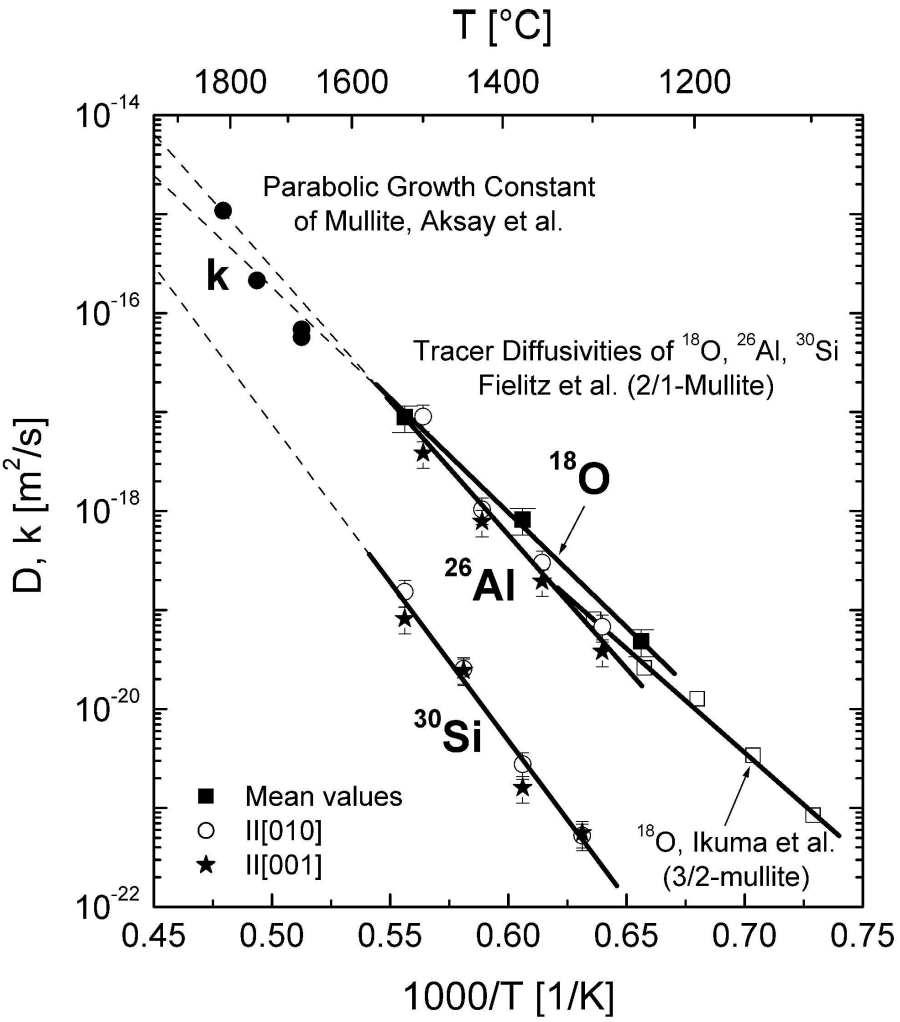

743x819mm (150 x 150 DPI)

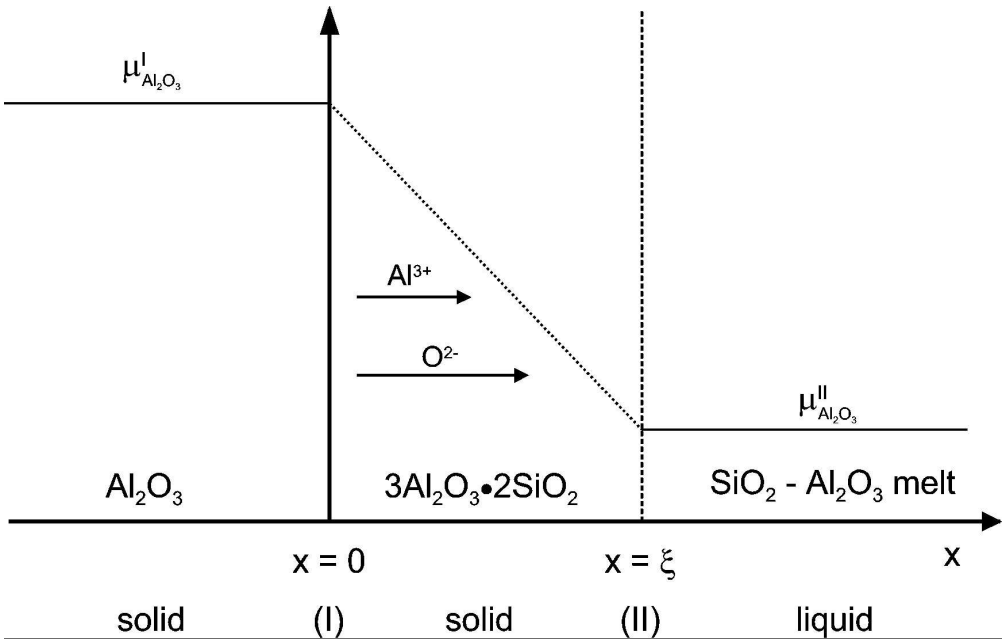

147x92mm (600 x 600 DPI)

Philosophical Magazine, submitted, revised

A diffusion-controlled mullite formation reaction model being based on tracer diffusivity data of aluminium, silicon and oxygen

P. FIELITZ*†, G. BORCHARDT†, M. SCHMÜCKER‡ and H. SCHNEIDER‡

†Institut für Metallurgie, Technische Universität Clausthal,
D-38678 Clausthal-Zellerfeld, Germany

‡Institut für Werkstoff-Forschung, Deutsches Zentrum für Luft- und Raumfahrt,
D-51147 Köln, Germany

* corresponding author: e-mail: peter.fielitz@tu-clausthal.de
phone: +49/5323/72-2634
fax: +49/5323/72-3184

This paper compiles all data of our tracer diffusivity studies in single crystalline 2/1-mullite. As tracers we used the rare stable isotopes ^{18}O and ^{30}Si and the artificial pseudo-stable isotope ^{26}Al. Secondary Ion Mass Spectrometry was applied to analyse the depth distribution of the tracer isotopes after the diffusion annealing. An essential result of our tracer diffusivity studies was the very low diffusivity of ^{30}Si compared to the diffusivities of ^{26}Al and ^{18}O, which are almost equal. Based on this observation we propose a reaction model for the diffusion-controlled mullite formation in the solid state, which assumes that the growth kinetics of a mullite layer is mainly controlled by the diffusion of aluminium ions and oxygen ions.

Keywords: mullite; tracer diffusion; formation reaction model

1. Introduction

Mullite is one of the most widely studied ceramic materials. This is due to its high thermal and chemical stability, good thermal shock behaviour and high creep resistance, which makes mullite a promising candidate for many high-temperature applications [1]. The crystal structure of mullite can be described as a modified defect structure of sillimanite ($Al_2O_3 \bullet SiO_2$). Sillimanite consists of edge-sharing aluminium-oxygen octahedral chains which are interconnected by double chains of ordered SiO_4 and AlO_4 tetrahedra. In mullite, the AlO_4-SiO_4-sequence is almost random [2] and there exists a certain amount of structural oxygen vacancies. The composition of mullite can be expressed as $Al_2^{VI}(Al_{2+2x}^{IV}Si_{2-2x})O_{10-x}$ where x indicates the amount of missing oxygen with respect to sillimanite and VI and IV indicate sixfold (octahedral) and fourfold (tetrahedral) coordination of aluminium ions. Silicon ions occupy tetrahedral sites only.

Sintering, grain growth, creep and all types of reconstructive reaction processes are strongly controlled by atomic diffusion. Therefore, the diffusivities of oxygen and silicon in single crystalline 2/1-mullite have been carefully determined in previous work using the rare natural isotopes ^{18}O and ^{30}Si as tracer isotopes [3], [4]. Secondary Ion Mass Spectrometry (SIMS) was applied to analyse the depth distribution of the tracer isotopes after the diffusion annealing. Recently, we applied the SIMS technique also to measure the diffusivity of aluminium in single crystalline 2/1-mullite using the pseudo-stable isotope ^{26}Al [5] so that we can now present a complete set of tracer diffusivity data (^{18}O, ^{30}Si, ^{26}Al) of all components of the mullite structure. Based on the results of these tracer diffusivity studies a reaction model for the diffusion controlled mullite formation is discussed in the following.

2. Experimental data

For all tracer diffusion experiments single crystalline 2/1 mullite disks (≈ 1 mm thick) cut perpendicular to [010] and [001] were used to measure the tracer diffusivities along the crystallographic b and c axes. The single crystals were synthesized by Dr. W. Walraffen (Univ. Bonn, Germany) using the Czochralski technique. Details of the crystal growth procedure were published by Guse and Mateika [6].

The b and c axes are very different from a crystallographic point of view, because the mullite structure consists of chains of edge-sharing AlO_6 octahedra running parallel to the crystallographic c axis. These AlO_6 chains are cross-linked by (Al, Si)O_4 tetrahedra forming

double chains, which also run parallel to c [1]. Therefore, a pronounced anisotropy of the diffusivities of the constituents could not be excluded a priori. However, all experimental tracer diffusivity data display virtually no orientation-dependent variation. The slight difference between b and c axes falls into the estimated error range of ± 30 % of diffusion data gained by the method of SIMS depth profiling. Therefore, all evaluated Arrhenius relations represent average values deduced from the diffusivity measurements along the two axes. Since structural arrangements along the a and b axes are very similar in mullite, tracer diffusivities parallel to both directions should also be in a comparable range. So it may be justified to consider tracer diffusivities of the components to be isotropic in mullite.

- Oxygen tracer diffusion

Oxygen diffusion is well studied in many oxides because it can be measured relatively simply by gas/solid exchange experiments [7]. We performed ^{18}O isotope exchange experiments on single crystalline 2/1-mullite samples [3] and obtained the following Arrhenius relation:

$$D_{18O}^{2/1} = (3.71\,^{+13}_{-3}) \times 10^{-5}\,\frac{m^2}{s}\exp\left(-\frac{(433 \pm 21)\,kJ/mol}{RT}\right) \quad (1)$$

In 3/2-mullite, Ikuma et al. [8] evaluated the ^{18}O tracer diffusivity indirectly on micrometer size single crystals by measuring the concentration of $^{18}O_2$ in the gas phase:

$$D_{18O}^{3/2} = (1.32 \pm 0.39) \times 10^{-6}\,\frac{m^2}{s}\exp\left(-\frac{(397 \pm 45)\,kJ/mol}{RT}\right) \quad (2)$$

- Silicon tracer diffusion

In contrast to oxygen, the measurement of silicon diffusivities in oxides is much more difficult. The complications arise from the fact that the natural tracer isotope ^{30}Si has a relatively high natural abundance of about 3.1 %. This circumstance limits the useful diffusion length and requires a deposition technique that allows to prepare very smooth ^{30}Si containing layers on the surface of the specimen. A detailed description of the experimental procedure is given in [4]. The following Arrhenius relation was obtained for the diffusivity of ^{30}Si in single crystalline 2/1-mullite:

$$D_{30Si}^{2/1} = (7.3\,^{+108}_{-6.8}) \times 10^{-2}\,\frac{m^2}{s}\exp\left(-\frac{(612 \pm 39)kJ/mol}{RT}\right) \quad (3)$$

- Aluminium tracer diffusion

Aluminium has no natural tracer isotopes and there are only a few aluminium diffusion data in the literature measured by means of the radiotracer isotope ^{26}Al [9]-[13]. The reason is that

two difficulties are encountered with this radiotracer. Firstly, ^{26}Al is artificial and causes very high production costs, and secondly, it has a half-life time of 7.4×10^5 years with a very low specific activity which makes it difficult to apply classical radiotracer methods [12]. The application of SIMS avoids the problems related to the radioactivity measurement, reduces the necessary amount of ^{26}Al per experiment considerably, and yields a much higher spatial resolution. A detailed description of the measurement of the ^{26}Al diffusivity in 2/1- mullite by means of the SIMS technique is given in [5]. For the diffusivity of ^{26}Al in single crystalline 2/1-mullite we obtained the following Arrhenius relation:

$$D^{2/1}_{26Al} = (9.2\ ^{+92}_{-8.4})\times10^{-3}\ \frac{m^2}{s}\exp\left(-\frac{(517\pm33)kJ/mol}{RT}\right) \quad (4)$$

[*Insert Fig. 1 about here*]

Fig. 1 shows our measured tracer diffusivities (^{18}O, ^{26}Al, ^{30}Si) in single crystalline 2/1-mullite and the ^{18}O diffusivity in single crystalline 3/2-mullite measured by Ikuma et al. [8]. There is only a small difference between the ^{18}O diffusivity in 2/1-mullite and 3/2-mullite. One observes that the diffusivity of ^{30}Si is much lower than the diffusivity of ^{18}O and ^{26}Al. Jaoul et al. [14] and Andersson et al. [15] measured ^{30}Si diffusivities in single crystalline forsterite Mg_2SiO_4 along three crystallographic directions. Both observed that in this silicate, too, silicon diffuses more slowly than oxygen and found no significant anisotropy of the diffusion coefficients. It is assumed that the strong covalent bond within the SiO_4 tetrahedron is an explanation for the low diffusivity of silicon. Furthermore, one observes from Fig. 1 that the diffusivity of ^{26}Al is comparable to the diffusivity of ^{18}O. Le Gall et al. [12] reported a similar result for the diffusivities of ^{26}Al and ^{18}O in single crystalline α-Al_2O_3.

The solid points in Fig. 1 at higher temperatures are experimental data of the parabolic growth constant, k, of diffusion-controlled mullite formation, intensively investigated by Aksay et. al [16], [17]. The quoted authors used diffusion couples made from sapphire and aluminium-silicate glasses of 10.9, 22.8, and 42.2 wt % Al_2O_3. These binary glasses are in equilibrium with mullite at 1678°C, 1753°C, and 1813°C. Thus, sapphire-glass diffusion couples of these compositions at the corresponding annealing temperatures could be used to study the growth kinetics of mullite as an intermediate phase without solution of mullite in the liquid glass

phase. The thickness of the mullite layer increased linearly with the square root of time, indicating that the growth mechanism is diffusion-controlled. The results of Aksay's experiments are outlined in Table 1.

[*Insert Table 1 about here*]

The dashed lines in Fig. 1 are extrapolated tracer diffusivity data from lower temperatures. This means, we know the tracer diffusivities of all components of mullite and the question arises how the measured parabolic growth constants are related to our measured tracer diffusivities. To answer this interesting question we will propose a reaction model for the diffusion-controlled mullite formation in the next chapter.

3. Reaction model

Sung [18] proposed a diffusion-controlled reaction model which is based on the assumption that the oxygen mobility is much lower than the mobility of the cations in mullite. Our tracer diffusion experiments show, however, that silicon is the slowest species compared to oxygen and aluminium in single crystalline 2/1-mullite. This is most probably also valid for 3/2-mullite (s. [8] for the diffusivity of ^{18}O in 3/2-mullite, which is virtually identical to the oxygen diffusivity in 2/1-mullite, as shown in Fig. 1). We will use our experimental observation to derive a more realistic reaction model which is schematically represented in Fig. 2.

[*Insert Fig. 2 about here*]

Because of the low silicon tracer diffusivity we neglect Si^{4+} ion fluxes and consider a formation mechanism where Al_2O_3 is transported by Al^{3+} and O^{2-} ion fluxes through the mullite layer. The fluxes are described by a coordinate system which is fixed to the phase boundary I. Such a coordinate system becomes applicable when one cation has a much lower mobility than other species [19]. The intrinsic drift velocity, $d\xi/dt$, describes the drift velocity of phase boundary II relative to phase boundary I. A simple, but fundamental, relation between the Al^{3+} and O^{2-} fluxes in Fig. 2 is given in the absence of space charges

$$3\,j_{Al^{3+}} - 2\,j_{O^{2-}} = 0 \tag{5}$$

In the literature (p. 229 in [20]) one finds the concept of a molecular flux, $j_{A_\alpha B_\beta}$, and a molecular diffusion coefficient, $D_{A_\alpha B_\beta}$, which is used to express the fact that the process takes places as if an entity $A_\alpha B_\beta$ of fixed composition (a "molecule" or better a "formula unit") were migrating. The condition for a molecular flux of Al_2O_3 is

$$j_{Al_2O_3} = \frac{j_{Al^{3+}}}{2} = \frac{j_{O^{2-}}}{3} \tag{6}$$

where j_i is the flux of the ion i (Al^{3+}, O^{2-}). Equation (6) ensures the composition to remain constant and is identical to equation (5) which excludes any build-up of space charge. That is, one can describe the two coupled Al^{3+} and O^{2-} ion fluxes by a single molecular flux of Al_2O_3

$$j_{Al_2O_3} = -\frac{c_{Al_2O_3} D_{Al_2O_3}}{RT} \frac{d\mu_{Al_2O_3}}{dx} \tag{7}$$

were c is the molecular concentration, D the molecular (ambipolar) diffusion coefficient and μ the molecular chemical potential of Al_2O_3 in the solid mullite layer. In ceramics the term ambipolar diffusion coefficient is preferred as it implies the fact of the migration of coupled charges (p. 232 in [20] or p. 238 in [21]). For the ambipolar diffusion coefficient of Al_2O_3 in equation (7) one gets after a lengthy calculation (see appendix A.1)

$$\frac{1}{D_{Al_2O_3}} = \frac{2}{D_{Al^{3+}}} + \frac{3}{D_{O^{2-}}} \tag{8}$$

where D_i is the diffusion coefficient of the ion i (Al^{3+}, O^{2-}) which is related to the random thermal motion of the ions. In diffusional transport the random thermal motion is superposed on a drift resulting from field forces like the gradient of the chemical potential. Using equation (7) one gets for the average drift velocity of Al_2O_3

$$v_{Al_2O_3} = \frac{j_{Al_2O_3}}{c_{Al_2O_3}} = -\frac{D_{Al_2O_3}}{RT} \frac{d\mu_{Al_2O_3}}{dx} \tag{9}$$

Since the forces ($d\mu_{Al_2O_3}/dx = 2\,d\mu_{Al^{3+}}/dx + 3\,d\mu_{O^{2-}}/dx$) are small on the atomic length scale, diffusion coefficients established under equilibrium conditions (i.e., vanishing forces) can be used to describe the drift of the ions (p. 107 in [22]).

The relation of the self diffusion coefficients, D_i, of the ions in equation (8) to our measured tracer diffusivities, D_{*i}, is given by $D_{*i} = f_{*i} D_i$, where f_{*i} is the so-called correlation factor (p. 97 in [20]). Correlation factors for self diffusion are calculated for different diffusion mechanisms and crystal structures and are often in the order of 1 (p. 98 in [20]). Therefore, we can calculate the ambipolar diffusion coefficient of Al_2O_3 in a first order approximation by our measured tracer diffusivities

$$\frac{1}{D_{Al_2O_3}} = \frac{2 f_{^{26}Al}}{D_{^{26}Al}} + \frac{3 f_{^{18}O}}{D_{^{18}O}} \cong \frac{2}{D_{^{26}Al}} + \frac{3}{D_{^{18}O}} \qquad (10)$$

Correlation effects diminish the effectiveness of atomic jumps ($f_{*i} \leq 1$) in diffusional random motion (p. 110 in [22]), that is, ambipolar diffusion coefficients calculated by our tracer diffusivities are lower limits.

To calculate the parabolic growth constant, k, it is assumed that the ion fluxes are quasi-steady which means that during a specific time interval the fluxes can be considered to be constant in space. Because the concentration of Al_2O_3 is practically constant inside the mullite layer the drift velocity of Al_2O_3 is also practically independent of x. Separating variables and integrating equation (9) between the phase boundaries I and II results in (p. 168 in [22])

$$v_{Al_2O_3} \xi = -\frac{1}{RT} \int_{(I)}^{(II)} D_{Al_2O_3} d\mu_{Al_2O_3} \qquad (11)$$

where ξ is the thickness of the mullite layer. The drift velocity of phase boundary II relative to phase boundary I is equal to the average drift velocity of the Al_2O_3 molecules, $d\xi/dt = v_{Al_2O_3}$, so that one calculates the parabolic growth constant, k, by separating variables and integrating equation (11)

$$k = \frac{\xi^2}{2t} = -\frac{1}{RT} \int_{(I)}^{(II)} D_{Al_2O_3} d\mu_{Al_2O_3} \qquad (12)$$

To integrate the right hand side of equation (12) we must know the dependence of the ambipolar diffusion coefficient on the chemical potential which requires the application of an appropriate defect model.

Aksay et al. [17] used diffusion couples with sapphire and aluminium-silicate glasses at different temperatures. For every temperature, the Al_2O_3 concentration of the binary glass was chosen so that the glass phase was in equilibrium with the mullite phase. That is, any growth of the mullite layer requires Al_2O_3 to be transported through the mullite layer from the

sapphire sample side. This transport is enabled by a flux of freely migrating defects which are formed during the mullite formation reaction. We assume that during the reaction of "SiO_2" from the binary glass with "Al_2O_3", which is located on regular sites in the mullite structure, aluminium vacancies and oxygen vacancies are formed according to the following reaction (applying the Kröger-Vink notation)

$$2\,SiO_2 + 6\,Al_{Al}^{\times} + 9\,O_O^{\times} = 6\,V_{Al}^{'''} + 9\,V_O^{\bullet\bullet} + Al_6Si_2O_{13} \qquad (13)$$

where $Al_6Si_2O_{13}$ is 3/2-mullite. If local defect equilibrium is assumed one gets from equation (13) the defect equilibrium constant

$$K_d = \frac{a_{V_{Al}^{'''}}^{6}\, a_{V_O^{\bullet\bullet}}^{9}}{a_{SiO_2}^{2}} \qquad (14)$$

where a_i is the activity of the species i (SiO_2, aluminium vacancies, oxygen vacancies). Furthermore, we assume that the dilution of the vacancies is sufficient to express activities by concentrations, $a_V \cong [V]$. Using the condition for electroneutrality, $3[V_{Al}^{'''}] = 2[V_O^{\bullet\bullet}]$, one gets from equation (14) a dependence of the vacancy concentration from the SiO_2 activity

$$[V_{Al}^{'''}] = \alpha\, a_{SiO_2}^{2/15} \quad \text{and} \quad [V_O^{\bullet\bullet}] = \frac{3}{2}\alpha\, a_{SiO_2}^{2/15} \quad \text{with} \quad \alpha \equiv \left(\frac{2}{3}\right)^{-3/5} K_d^{1/15} \qquad (15)$$

If the diffusivity of aluminium ions is proportional to the concentration of aluminium vacancies, $D_{Al^{3+}} \propto [V_{Al}^{'''}]$, and if the diffusivity of oxygen ions is proportional to the concentration of oxygen vacancies, $D_{O^{2-}} \propto [V_O^{\bullet\bullet}]$, one can conclude from equations (8) and (15) that the ambipolar diffusion coefficient of Al_2O_3 is proportional to $a_{SiO_2}^{2/15}$

$$D_{Al_2O_3} = D_{Al_2O_3}^{I}\left(\frac{a_{SiO_2}}{a_{SiO_2}^{I}}\right)^{2/15} \qquad (16)$$

where the superscript I denotes values at the phase boundary I. Inserting equation (16) into equation (12) gives after some calculations (see appendix A.2)

$$k = n\,(D_{Al_2O_3}^{II} - D_{Al_2O_3}^{I}) \quad \text{with} \quad n = 5 \qquad (17)$$

where the superscripts I and II denote values of the ambipolar diffusion coefficient at the corresponding phase boundaries in Fig. 2.

4. Discussion

The calculations in chapter 3 show that the parabolic growth constant, k, is proportional to the difference of the ambipolar diffusion coefficients of Al_2O_3 at the phase boundaries (see equation (17)) where the calculated proportional constant, n, depends on the applied defect model and is 5 for the proposed one (equation (13)). It is interesting to note that only the difference of the absolute values of the ambipolar diffusion coefficients plays a role for the diffusion controlled growth kinetics of the reaction layer (mullite). The absolute values of the ambipolar diffusion coefficients of Al_2O_3 at both phase boundaries are determined by the freely migrating defects which are formed during the mullite formation reaction. Equation (17) would be the most direct way to calculate parabolic growth constants from diffusivity data. However, this procedure requires the same defect chemistry to be valid for the entire composition range of mullite and it requires the measurements of the two diffusion constants.

Because diffusivity measurements are often only possible at one of the two interfaces it is useful to express equation (17) by

$$k = D^{I}_{Al_2O_3} \Delta R \tag{18}$$

with the dimensionless factor

$$\Delta R = n \frac{D^{II}_{Al_2O_3} - D^{I}_{Al_2O_3}}{D^{I}_{Al_2O_3}} \tag{19}$$

where we have assumed that the ambipolar diffusion coefficient of Al_2O_3 at phase boundary I corresponds to our calculated ambipolar diffusion coefficient of Al_2O_3 from the measured tracer diffusivity data. The disadvantage of this notation is that it seems to suggest that $D^{I}_{Al_2O_3}$ and the dimensionless factor, ΔR, are independent terms, with the wrong implication that k is proportional to the absolute value of $D^{I}_{Al_2O_3}$. The advantage of this notation will, however, become obvious in the development given below.

The diffusivities at the interfaces are proportional to the freely migrating defects at the interfaces so that one gets for the dimensionless factor ΔR (considering equations (15) and (16))

$$\Delta R = n \frac{[V'''_{Al}]^{II} - [V'''_{Al}]^{I}}{[V'''_{Al}]^{I}} = n \frac{[V^{\bullet\bullet}_{O}]^{II} - [V^{\bullet\bullet}_{O}]^{I}}{[V^{\bullet\bullet}_{O}]^{I}} \tag{20}$$

As ΔR is proportional to the relative change of the concentrations of the transporting defects it

can be calculated from our proposed defect model (see appendix A.3)

$$\Delta R = 5\left[(a^{II}_{SiO_2})^{\frac{2}{15}} \exp\left(-\frac{\Delta_r G^{\circ}_{Al_6Si_2O_{13}}}{15\,RT}\right) - 1\right] \tag{21}$$

where $\Delta_r G^{\circ}_{Al_6Si_2O_{13}}$ is the Gibbs free energy for the formation of 3/2-mullite from the parent oxides and $a^{II}_{SiO_2}$ is the activity of SiO_2 in the aluminium-silicate melt at phase boundary II.

In the absence of any plausible defect model one could assume, as a first approximation, a constant diffusion coefficient, $D_{Al_2O_3} = D^{I}_{Al_2O_3} = D^{II}_{Al_2O_3}$, which allows the simplest integration of the right hand side of equation (12). This gives

$$k_0 = D^{I}_{Al_2O_3}\,\Delta R_0 \tag{22}$$

with the dimensionless factor ΔR_0

$$\Delta R_0 = \frac{\left|\Delta\mu_{Al_2O_3}\right|}{RT} \quad \text{and} \quad \Delta\mu_{Al_2O_3} = \mu^{II}_{Al_2O_3} - \mu^{I}_{Al_2O_3} \tag{23}$$

where the superscripts I and II denote values of the chemical potential of Al_2O_3 at the corresponding phase boundaries in Fig. 2 and the subscript 0 indicates values of a first approximation. The difference of the chemical potential of Al_2O_3 at both phase boundaries can be calculated by means of the Gibbs free energy of formation of 3/2-mullite from the oxides and the activity of SiO_2 in the aluminium-silicate melt at phase boundary II (see appendix A.4).

$$\Delta\mu_{Al_2O_3} = \frac{\Delta_r G^{\circ}_{Al_6Si_2O_{13}}}{3} - \frac{2}{3}RT\ln(a^{II}_{SiO_2}) \tag{24}$$

[*Insert Table 2 about here*]

The dimensionless factors ΔR_0 and ΔR for the 3/2-mullite formation from the oxides are calculated in Table 2 for experimental temperatures used by Aksay et. al [17] (see Table 1). It is obvious that both factors are practically equal in this temperature range. Comparing equations (18) and (22) through the ratio

$$\frac{k}{k_0}=\frac{\Delta R}{\Delta R_0}=\frac{5\left[\left(a_{SiO_2}^{(II)}\right)^{\frac{2}{15}}\exp\left(-\frac{\Delta_r G^{\circ}_{Al_6Si_2O_{13}}}{15RT}\right)-1\right]}{-\frac{\Delta_r G^{\circ}_{Al_6Si_2O_{13}}}{3RT}+\frac{2}{3}\ln(a_{SiO_2}^{(II)})} \qquad (25)$$

one can conclude that the reason for this observation is the low value of the Gibbs free energy, $\Delta_r G^{\circ}_{Al_6Si_2O_{13}} \approx -35\,kJ/mol$, for the formation of 3/2-mullite from the oxides and the high experimental temperatures, $RT \approx 17\,kJ/mol$. Therefore, our proposed defect model does practically not improve the agreement between the experimental data and the calculated parabolic growth rates in this temperature range, so that it is not meaningful to try a quantitatively validation of this model. It is, however, extremely useful to discuss this phenomenon from a more general point of view. The derivation of the factor of first approximation, ΔR_0, starts with the assumption that the (chemical) diffusion coefficient, D, in the reaction layer is practically constant and we assume, of course, that the calculated parabolic growth rate is practically correct, which implies the approximate relation

$$\frac{\Delta R_0}{n}\approx\frac{\Delta R}{n} \quad \text{if} \quad D\approx \text{constant} \qquad (26)$$

where n is a correct number evaluated from a correct defect model. Considering equations (23) and (19) we can express relation (26) by

$$\left|\frac{\Delta\mu_i}{nRT}\right|\approx\left|\frac{D_i^{II}-D_i^{I}}{D_i^{I}}\right| \quad \text{if} \quad D\approx \text{constant} \qquad (27)$$

where $i = Al_2O_3$ for the proposed mullite formation reaction. Such a relation holds for all formation reactions which can be treated mathematically in the same formal manner.

The right hand side of relation (27) corresponds to the relative change of the diffusivity across the mullite layer. That is, the assumption that the diffusion coefficient in the reaction layer is practically constant is fulfilled if $|\Delta\mu_i| < |n|RT$. This case is generally more likely at higher temperatures and reactions with low Gibbs free energy of formation (e.g the considered mullite formation from the oxides). One has then $\Delta R_0 \approx \Delta R$ and can calculate the parabolic growth constant by the simple equation (22). The application of a defect model does practically not improve the calculated parabolic growth constants in the considered temperature range so that it becomes difficult to prove a proposed defect model quantitatively from experimentally determined parabolic

growth constants.

The case $|\Delta\mu_i| > |n|RT$ is clearly in conflict with relation (27) which is based on the assumption that the diffusion coefficient in the reaction layer is approximately constant. This case is generally more likely at lower temperatures and reactions with high Gibbs free energy of formation. It is then not reasonable to assume a constant diffusion coefficient to integrate equation (12), so that an appropriate defect model is necessary to calculate parabolic growth constants.

The measured parabolic growth rates of 3/2-mullite are by a factor of 4 to 17 larger (see the ratio k_{exp}/k_{calc} in Table 2) than the parabolic growth rates calculated from our measured tracer diffusivities in single crystalline 2/1-mullite. Two terms were used to calculate the theoretical parabolic growth rates (see equation (18)): a diffusivity term and a dimensionless term, the factor, ΔR, which could be expressed in a good approximation by the normalised change of the chemical potential of Al_2O_3, $|\Delta\mu_{Al_2O_3}|/RT$, across the reaction layer. Hence, a strong deviation from the experimental values cannot be explained by a wrong calculation of the factor, ΔR, because this would imply a very erroneous calculation of the chemical potential of Al_2O_3. The observed deviation from the experimental values must be induced by the calculation of the diffusivity term in equation (18). This term was calculated by equation (10) using our measured bulk tracer diffusivities. As we mentioned above the use of tracer diffusivities, and neglecting correlation effects, will result principally in a lower limit value of the diffusivity term in equation (18). Furthermore, grain boundary diffusion has to be considered to explain why the diffusivities of the oxygen ions and the aluminium ions during the mullite formation are significantly higher than our measured bulk tracer diffusivities.

Grain boundary tracer diffusivities of mullite are known for the ^{18}O isotope only [23]. In the grain boundaries a much higher ^{18}O diffusivity (up to a factor of 10^4) was observed than in the bulk. The amount of Al_2O_3 which is transported through the grain boundaries is proportional to the volume fraction of grain boundaries in the mullite layer. Therefore, an effective diffusion coefficient can be calculated by the Hart-Mortlock equation [24][25]

$$D_{eff} = s\,g\,D_{gb} + (1 - s\,g)\,D \qquad (28)$$

where D is the bulk diffusivity, D_{gb} the grain boundary diffusivity, g the volume fraction of grain boundaries, and s the grain boundary segregation factor ($s = 1$ for self-diffusion). Assuming a similar enhancement (a factor of 10^4) of the ^{26}Al diffusivities in the grain

boundaries one can conclude from the Hart-Mortlock equation that volume fractions of grain boundaries from 2.9×10^{-4} to 1.6×10^{-3} are sufficient to explain the observed discrepancies between calculated and measured parabolic growth rates. For a cubic grain geometry one can estimate the grain size, d, by $d \approx 3\delta / g$ (p. 206 in [26]). Assuming an average grain boundary width δ = 1 nm one gets corresponding cubic grain sizes from 10 µm to 2 µm.

This explanation is plausible, however, the larger discrepancy at higher temperatures is somewhat contradictory to conventional thinking about grain boundary effects (i.e., the relative contribution from grain boundary diffusion is often larger at lower temperatures). Another explanation could be impurity effects on diffusion, even with relatively pure starting materials. For example, one observes a scatter band of about one order of magnitude for measured oxygen diffusivities in nominally undoped α-Al_2O_3 which is mainly explained by impurities which induce extrinsic point defects and affect the diffusion process [27]. Furthermore, we have assumed that the influence of the Si/Al ratio does not strongly affect the diffusion process. This assumption is based on the low value of the Gibbs free energy of formation of mullite and on the resulting close agreement of the oxygen diffusivity data obtained for (single crystalline) 2/1-mullite and 3/2-mullite (see also [28] for further discussion) but is open to debate for the aluminium diffusivity.

This discussion shows that the parabolic growth rates calculated from our measured bulk tracer diffusivity data of oxygen and aluminium define at least a lower limit of the experimentally observed growth rates. With the exception of the mullite formation data set at the highest temperature (1813 °C) the discrepancy between parabolic rate constants calculated on the basis of (extrapolated) bulk diffusion data and the experimentally determined rate constants is about half an order of magnitude, which clearly supports our model, taking into account that the details of the growth experiment (impurity concentrations etc.) are not fully evident from the literature.

5. Summary

An essential result of our tracer diffusivity studies in single crystalline 2/1-mullite is the very low diffusivity of ^{30}Si compared to the diffusivities of ^{26}Al and ^{18}O, which are almost equal. Based on this observation we propose a diffusion-controlled mullite formation model which assumes that the growth kinetics of a mullite layer is controlled by the diffusion of aluminium

ions and oxygen ions. The two ionic fluxes can be described by a single molecular (ambipolar) flux of Al_2O_3 which transports Al_2O_3 through the mullite layer and reacts with SiO_2 to mullite. The ambipolar flux of Al_2O_3 is enabled by freely migrating defects which are formed during the mullite formation reaction.

The reaction of SiO_2 with Al_2O_3 on regular sites in the mullite structure requires the formation of aluminium vacancies and oxygen vacancies (equation (13)). Based on this defect model we derive equation (17) to calculate the parabolic growth constant of mullite formation. However, the direct application of this equation requires the proposed defect model to be valid in the whole mullite layer and necessitates the measurement of tracer diffusivities at the two interfaces. Therefore, we write equation (17) into the form of equation (18) by the definition of a dimensionless factor, ΔR, and assume that the ambipolar diffusion coefficient of Al_2O_3 at interface I corresponds to the ambipolar diffusion coefficient of Al_2O_3 calculated from our tracer diffusivity data. The factor, ΔR, is then calculated by means of the proposed defect model (see equation (21)).

Further, it is demonstrated that because of the fairly low value of the Gibbs free energy of formation of mullite the ambipolar diffusion coefficient of Al_2O_3 in the mullite layer is practically constant.

To calculate the parabolic growth rate of mullite formation we need the ambipolar diffusion coefficient of Al_2O_3 in the mullite layer which can principally be calculated from the diffusion coefficients of aluminium and oxygen (equation (8)). Neglecting correlation effects we calculate the ambipolar diffusion coefficient of Al_2O_3 from our measured tracer diffusivity data (equation (10)). **The results of this calculation are compiled in Table 2 and show that our calculated values are about a factor of 5 lower than the measured values by Aksay et al. [17], at least below 1750 °C. Taking into account typical experimental errors in layer growth experiments this fairly small discrepancy supports our reaction model. Our calculated values thus define a lower limit of the parabolic growth rate.**

Acknowledgement

Financial support from Deutsche Forschungsgemeinschaft (DFG) is gratefully acknowledged. **The comments of an anonymous reviewer helped to improve the manuscript.**

Appendix A

For the following derivations it is assumed that local thermodynamical equilibrium is maintained within the reaction layer and also at the phase boundaries I and II, so that the following equilibrium condition is valid

$$2\,Al^{3+} + 3O^{2-} = Al_2O_3 \tag{29}$$

$$2\eta_{Al^{3+}} + 3\eta_{O^{2-}} = \mu_{Al_2O_3} \tag{30}$$

where η is the electrochemical potential of electrically charged particles (Al^{3+}, O^{2-}) and μ is the chemical potential of the uncharged particle (Al_2O_3). The chemical reaction equation of the 3/2-mullite formation from the oxides is given by

$$2\,SiO_2 + 3\,Al_2O_3 = Al_6Si_2O_{13} \tag{31}$$

The reaction equilibrium constant, K_r, can be written as

$$K_r = \frac{a_{Al_6Si_2O_{13}}}{a^3_{Al_2O_3}\,a^2_{SiO_2}} = \exp\left(-\frac{\Delta_r G^\circ_{Al_6Si_2O_{13}}}{RT}\right) \tag{32}$$

where a_i is the activity of component i ($Al_6Si_2O_{13}$, Al_2O_3, SiO_2) and $\Delta_r G^\circ_{Al_6Si_2O_{13}}$ is the Gibbs free energy of formation of 3/2-mullite from the oxides which can be calculated by the free energy of the formation from elements, $\Delta_f G^\circ_i$ tabulated in [29] or [30],

$$\Delta_r G^\circ_{Al_6Si_2O_{13}} = \Delta_f G^\circ_{Al_6Si_2O_{13}} - 3\Delta_f G^\circ_{Al_2O_3} - 2\,\Delta_f G^\circ_{SiO_2} \tag{33}$$

The activity of 3/2-mullite is 1 in the mullite layer so that equation (32) yields

$$2\,RT\ln\left(a_{SiO_2}\right) + 3\,RT\ln\left(a_{Al_2O_3}\right) = \Delta_r G^\circ_{Al_6Si_2O_{13}} \tag{34}$$

A.1 Derivation of equation (8)

The fluxes of aluminium and oxygen ions are given by

$$j_{Al^{3+}} = -\frac{c_{Al^{3+}}\,D_{Al^{3+}}}{RT}\frac{d\eta_{Al^{3+}}}{dx}$$

$$j_{O^{2-}} = -\frac{c_{O^{2-}}\,D_{O^{2-}}}{RT}\frac{d\eta_{O^{2-}}}{dx} \tag{35}$$

where c_i, D_i and η_i are the concentration, the diffusion coefficient and the electrochemical

potential of the ion i (Al^{3+}, O^{2-}), respectively [31]. The gradient of the electrochemical potentials can be expressed by

$$\frac{d\eta_{Al^{3+}}}{dx} = \frac{d\mu_{Al^{3+}}}{dx} + 3F\frac{d\varphi}{dx}$$
$$\frac{d\eta_{O^{2-}}}{dx} = \frac{d\mu_{O^{2-}}}{dx} - 2F\frac{d\varphi}{dx} \qquad (36)$$

where F is the Faraday constant and φ the electrical potential. The condition for electroneutrality, equation (5), is used to eliminate the unknown term F×dφ/dx from the flux equations.

$$F\frac{d\varphi}{dx} = -\frac{3c_{Al^{3+}}D_{Al^{3+}}\frac{d\mu_{Al^{3+}}}{dx} - 2c_{O^{2-}}D_{O^{2-}}\frac{d\mu_{O^{2-}}}{dx}}{9c_{Al^{3+}}D_{Al^{3+}} + 4c_{O^{2-}}D_{O^{2-}}} \qquad (37)$$

Inserting equation (37) into the flux equations (35)-(36) and respecting equation (5) and (30) one gets for the ion fluxes

$$\frac{j_{Al^{3+}}}{2} = \frac{j_{O^{2-}}}{3} = -\frac{\langle cD\rangle_{Al_2O_3}}{RT}\frac{d\mu_{Al_2O_3}}{dx} \qquad (38)$$

with the shortcut

$$\langle cD\rangle_{Al_2O_3} \equiv \frac{c_{Al^{3+}}D_{Al^{3+}} \times c_{O^{2-}}D_{O^{2-}}}{9c_{Al^{3+}}D_{Al^{3+}} + 4c_{O^{2-}}D_{O^{2-}}} \qquad (39)$$

By equation (7) an ambipolar diffusion coefficient was defined. Comparing equations (6), (7) and (38) one concludes that the ambipolar diffusion coefficient is given by

$$D_{Al_2O_3} = \frac{\langle cD\rangle_{Al_2O_3}}{c_{Al_2O_3}} = \frac{D_{Al^{3+}}D_{O^{2-}}}{9(c_{Al_2O_3}/c_{O^{2-}})D_{Al^{3+}} + 4(c_{Al_2O_3}/c_{Al^{3+}})D_{O^{2-}}} \qquad (40)$$

and finally because of the concentration relations

$$c_{Al_2O_3} = \frac{c_{Al^{3+}}}{2} = \frac{c_{O^{2-}}}{3} \qquad (41)$$

one derives equation (8). Considering equation (6) and equation (41) one concludes

$$v = \frac{j_{Al_2O_3}}{c_{Al_2O_3}} = \frac{j_{Al^{3+}}}{c_{Al^{3+}}} = \frac{j_{O^{2-}}}{c_{O^{2-}}} \qquad (42)$$

Thus, all particles (Al_2O_3, Al^{3+}, O^{2-}) considered in the proposed mullite formation model migrate with the same drift velocity, v.

A.2 Derivation of equation (17)

By definition the chemical potential of Al_2O_3 is given by

$$\mu_{Al_2O_3} = \mu^{\circ}_{Al_2O_3} + RT\ln(a_{Al_2O_3}) \tag{43}$$

considering also equation (34) one can express equation (12) by

$$k = \frac{2}{3}\int_{(I)}^{(II)} D_{Al_2O_3}\, d\ln(a_{SiO_2}) = \frac{2}{3}\int_{(I)}^{(II)} \frac{D_{Al_2O_3}}{a_{SiO_2}}\, da_{SiO_2} \tag{44}$$

Inserting equation (16) gives

$$k = 5\frac{D^{I}_{Al_2O_3}}{(a^{I}_{SiO_2})^{2/15}}\left[(a^{II}_{SiO_2})^{2/15} - (a^{I}_{SiO_2})^{2/15}\right] = 5(D^{II}_{Al_2O_3} - D^{I}_{Al_2O_3}) \tag{45}$$

A.3 Derivation of equation (21)

The factor ΔR is defined by equation (18). Considering equations (45) and (16) gives

$$\Delta R = 5\left[\frac{(a^{II}_{SiO_2})^{2/15}}{(a^{I}_{SiO_2})^{2/15}} - 1\right] \tag{46}$$

At interface I the activity of Al_2O_3 is 1 (see Fig. 2) so that one can calculate the activity of SiO_2 at interface I using equation (34)

$$(a^{I}_{SiO_2})^{2/15} = \exp\left(\frac{\Delta G^{\circ}_{Al_6Si_2O_{13}}}{15RT}\right) \tag{47}$$

Inserting equation (47) into equation (46) gives equation (21).

A.4 Derivation of equation (24)

The activity of Al_2O_3 is 1 at interface I and $a^{II}_{Al_2O_3}$ at interface II (see Fig. 2) so that one gets from equation (43) for the difference of the chemical potential

$$\Delta\mu_{Al_2O_3} = \mu^{II}_{Al_2O_3} - \mu^{I}_{Al_2O_3} = RT\ln(a^{II}_{Al_2O_3}) \tag{48}$$

Considering equation (34) one gets equation (24).

References

[1] H. Schneider, K. Okada and J.A. Pask, *Mullite and Mullite Ceramics* (John Wiley & Sons Ltd., Chichester, 1994).

[2] M. Schmücker, K.J.D. MacKenzie, M.E. Smith, D.L. Carroll and H. Schneider, J. Am. Ceram. Soc. **88** 2935 (2005).

[3] P. Fielitz, G. Borchardt, M. Schmücker, H. Schneider, M. Wiedenbeck, D. Rhede, S. Weber and S. Scherrer, J. Am. Ceram. Soc. **84** [12] 2845 (2001).

[4] P. Fielitz, G. Borchardt, M. Schmücker and H. Schneider, Phys. Chem. Chem. Phys. **5** 2279 (2003).

[5] P. Fielitz, G. Borchardt, M. Schmücker and H. Schneider, Solid State Ionics (2006), in press.

[6] W. Guse and D. Mateika, J. Cryst. Growth **22** 237 (1974).

[7] P. Fielitz and G. Borchardt, Solid State Ionics **144** 71 (2001).

[8] Y. Ikuma, E. Shimada, S. Sakano, M. Oishi, M. Yokoyama and Z. Nakagawa, J. Electrochem. Soc. **146** 4672 (1999).

[9] A.E. Paladino and W.D. Kingery, J. Chem. Phys. **37** 957 (1962).

[10] M. Beyeler and Y. Adda, J. Physique **29** 345 (1968).

[11] L.N. Larikov, V.V. Geichenko and V.M. Fal'chenko, *Diffusion Processes in Ordered Alloys* (Amerind Publ. Co, New Delhi, 1981) pp. 111–121.

[12] M. Le Gall, B. Lesage and J. Bernardini, Phil. Mag. A **70** 761 (1994).

[13] G.H. Frischat, J. Am. Ceram. Soc. **52** 625 (1969).

[14] O. Jaoul, M. Poumellec, C. Froidevaux and A. Havette, in *Anelasticity in the Earth*, edited by F.D. Stacey et al. (Geodyn. Ser. Vol. 4, AGU, Washington, DC, 1981) pp. 95–100.

[15] K. Andersson, G. Borchardt, S. Scherrer and S. Weber, Fresenius Z. Anal. Chem. **333** 383 (1989).

[16] I.A. Aksay, Diffusion and Phase Relationship Studies in the Alumina-Silica System. PhD thesis, University of California, Berkeley (1973).

[17] I.A. Aksay and J.A. Pask, J. Am. Ceram. Soc. **58** [11-12] 507 (1975).

[18] Y.-M. Sung, Acta mater. **48** 2157 (2000).

[19] A.R. Cooper Jr. and J.H. Heasley, J. Am. Ceram. Soc. **49** [5] 280 (1966).

[20] J. Philibert, *Atom Movements - Diffusion and Mass Transport in Solids* (Les Éditions de Physique, Les Ulis Cedex A, 1991).

[21] Y.-M. Chiang, D.P. Birnie and W.D. Kingery, *Physical Ceramics: Principles for Ceramic Science and Engineering* (John Wiley & Sons, New York, 1997).

[22] H. Schmalzried, *Chemical Kinetics of Solids* (VCH, Weinheim, 1995).

[23] P. Fielitz, G. Borchardt, M. Schmücker, H. Schneider and P. Willich, J. Am. Ceram. Soc. **87** [12] 2232 (2004).

[24] E.W. Hart, Acta Metall. **5** 597 (1957).

[25] A.J. Mortlock, Acta Metall. **8** 132 (1960).

[26] I. Kaur, Y. Mishin, W. Gust, *Fundamentals of Grain and Interphase Boundary Diffusion* (John Wiley & Sons Ltd., Chichester, 1995).

[27] D. Prot and C. Monty, Phil. Mag. A **73** [4] 899 (1996).

[28] P. Fielitz, G. Borchardt, M. Schmücker and H. Schneider, J. Eur. Ceram. Soc. **21** 2577 (2001).

[29] I. Barin, *Thermochemical Data of Pure Substances* (Part I + II, VCH Publishers, Weinheim, 1989).

[30] M.W. Chase Jr., C.A. Davies, J.R. Downey Jr., D.J. Frurip, R.A. McDonald and A.N. Syverud, *JANAF Thermochemical Tables* (3rd ed., ACS, AIP, NBS, New York, 1986).

[31] H. Schmalzried, *Solid State Reactions* (2nd ed., Verlag Chemie, Weinheim, 1981).

Tables

Table 1 Experimental conditions and data for sapphire-equilibrium-melt runs [17], where t is the annealing time, ξ is the mullite layer thickness, and k_{exp} the experimental parabolic growth constant.

T °C	Melt mol % Al_2O_3	Mullite mol % Al_2O_3	t min	ξ µm	$k_{exp} = \xi^2/(2t)$ m^2/s
1678	6.75	58.6-62.7	12,182	10	6.8×10^{-17}
1678	6.75	58.6-62.7	47,380	18	5.7×10^{-17}
1753	14.9	58.6-62.7	6,608	13	2.1×10^{-16}
1813	30.2	59.9-62.7	10,025	36	1.1×10^{-15}

Table 2 Parabolic growth rates calculated from the measured tracer diffusivities of aluminium and oxygen using equations (10), (18) and (21) (compare with experimental data in Table 1). The activity of SiO_2 at phase boundary II, $a^{II}_{SiO_2}$, was approximated by the molar fraction of SiO_2 in the aluminium-silicate melt. The free energy, $\Delta_r G^\circ_{Al_6Si_2O_{13}}$, for the formation of 3/2-mullite from the oxides was calculated with equation (33) using thermochemical data from [29]. The dimensionless factor of first approximation, ΔR_0, was calculated by equations (23), (24).

T °C	RT kJ/mol	$\Delta_r G^\circ_{Al_6Si_2O_{13}}$ kJ/mol	$a^{II}_{SiO_2}$	ΔR_0	ΔR	$D_{Al_2O_3}$ m^2/s	k_{calc} m^2/s	k_{exp} / k_{calc}
1678	16.2	-33.8	0.93	0.65	0.69	2.1×10^{-17}	1.5×10^{-17}	4.6
1678	16.2	-33.8	0.93	0.65	0.69	2.1×10^{-17}	1.5×10^{-17}	3.9
1753	16.8	-35.3	0.85	0.59	0.63	6.1×10^{-17}	3.8×10^{-17}	5.6
1813	17.3	-36.5	0.70	0.46	0.48	1.3×10^{-16}	6.4×10^{-17}	17

Figure Captions

Fig. 1 Compilation of our measured tracer diffusivities (^{18}O, ^{26}Al, ^{30}Si) in single crystalline 2/1-mullite. Ikuma et al. [8] measured the ^{18}O diffusivity in single crystalline 3/2-mullite. Also shown are data of the parabolic growth constant, k, of mullite formation measured by Aksay et al. [17] via high-temperature diffusion couple experiments.

Fig. 2 Schematic representation of the reaction model for the mullite formation. Al_2O_3 is transported through the solid mullite layer by means of intrinsic Al^{3+} and O^{2-} ion fluxes and reacts to 3/2-mullite with SiO_2 from the aluminosilicate melt which is in equilibrium with mullite. The chemical potential of Al_2O_3 decreases across the mullite layer, the limiting values are $\mu^{I}_{Al_2O_3}$ in α-Al_2O_3 and $\mu^{II}_{Al_2O_3}$ in the aluminosilicate melt.

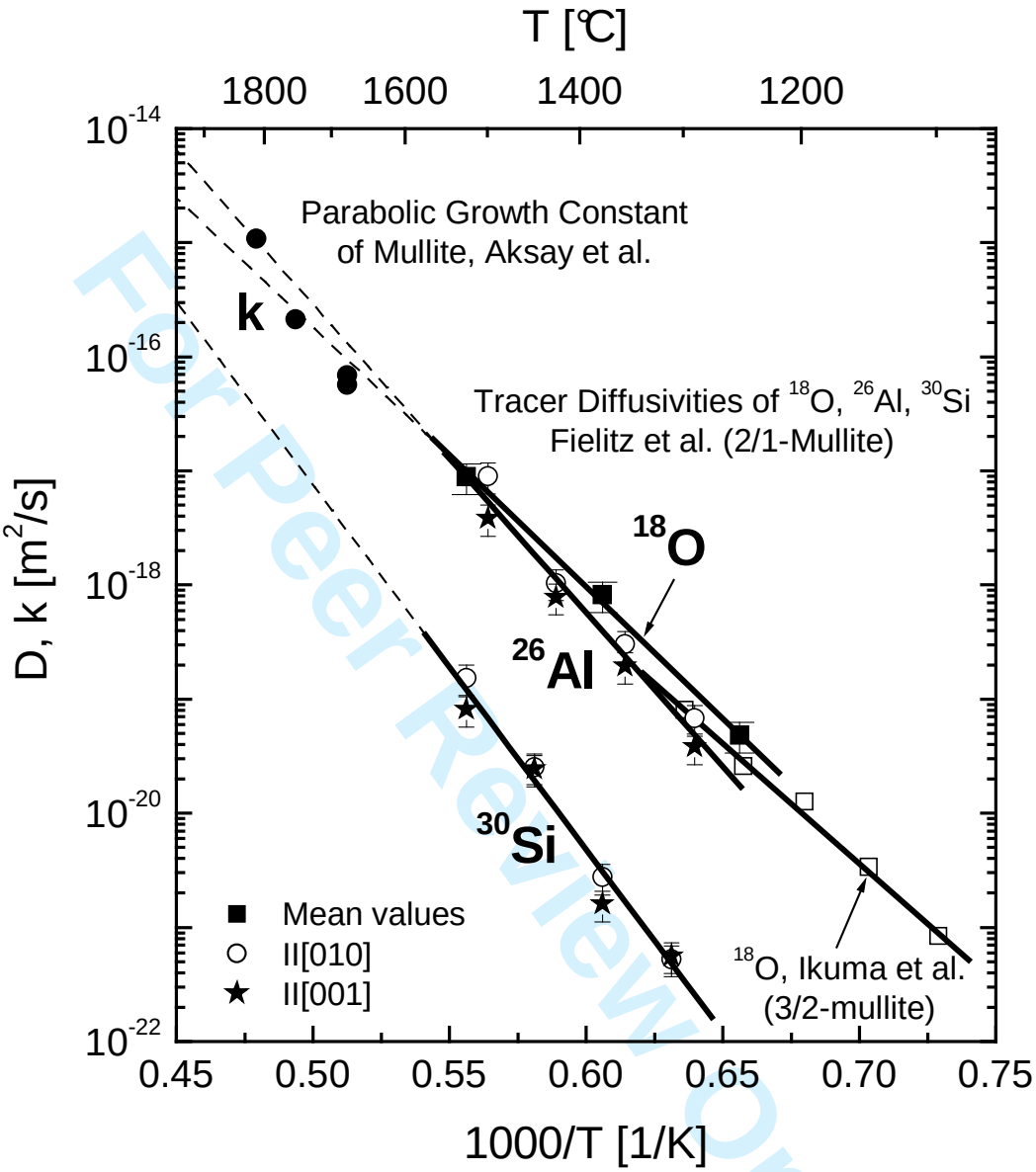

Fig. 1

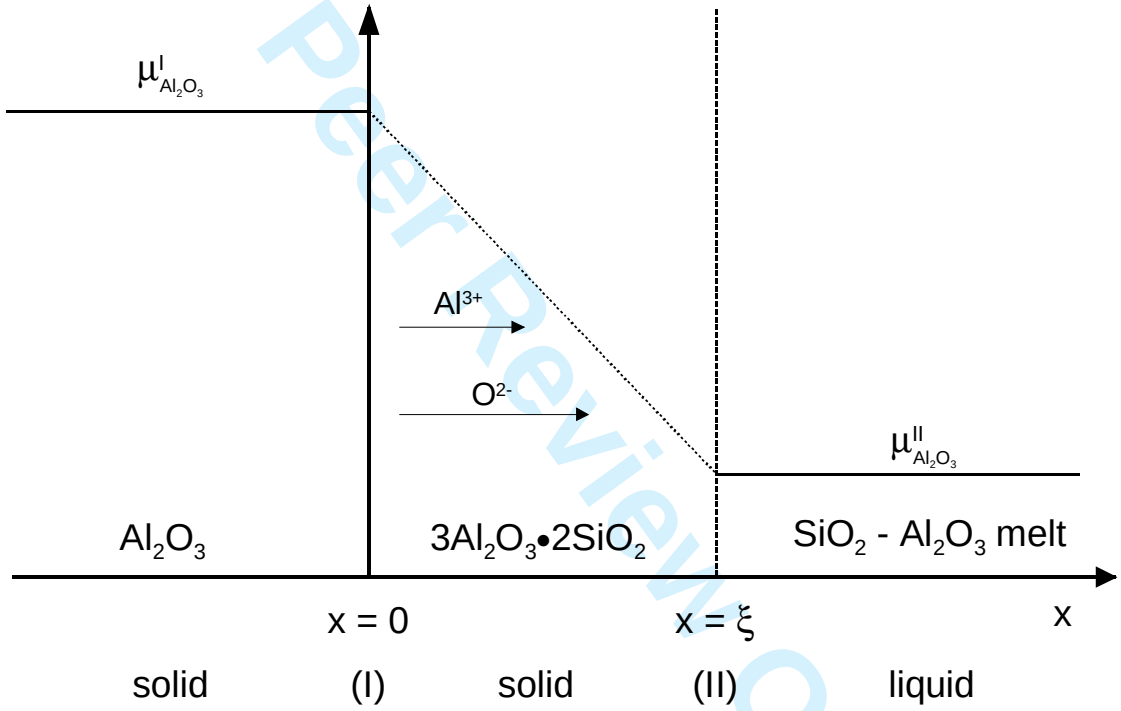

Fig. 2

Philosophical Magazine, submitted, revised

A diffusion-controlled mullite formation reaction model being based on tracer diffusivity data of aluminium, silicon and oxygen

P. FIELITZ*†, G. BORCHARDT†, M. SCHMÜCKER‡ and H. SCHNEIDER‡

†Institut für Metallurgie, Technische Universität Clausthal,
D-38678 Clausthal-Zellerfeld, Germany

‡Institut für Werkstoff-Forschung, Deutsches Zentrum für Luft- und Raumfahrt,
D-51147 Köln, Germany

* corresponding author: e-mail: peter.fielitz@tu-clausthal.de
phone: +49/5323/72-2634
fax: +49/5323/72-3184

This paper compiles all data of our tracer diffusivity studies in single crystalline 2/1-mullite. As tracers we used the rare stable isotopes ^{18}O and ^{30}Si and the artificial pseudo-stable isotope ^{26}Al. Secondary Ion Mass Spectrometry was applied to analyse the depth distribution of the tracer isotopes after the diffusion annealing. An essential result of our tracer diffusivity studies was the very low diffusivity of ^{30}Si compared to the diffusivities of ^{26}Al and ^{18}O, which are almost equal. Based on this observation we propose a reaction model for the diffusion-controlled mullite formation in the solid state, which assumes that the growth kinetics of a mullite layer is mainly controlled by the diffusion of aluminium ions and oxygen ions.

Keywords: mullite; tracer diffusion; formation reaction model

1. Introduction

Mullite is one of the most widely studied ceramic materials. This is due to its high thermal and chemical stability, good thermal shock behaviour and high creep resistance, which makes mullite a promising candidate for many high-temperature applications [1]. The crystal structure of mullite can be described as a modified defect structure of sillimanite ($Al_2O_3 \bullet SiO_2$). Sillimanite consists of edge-sharing aluminium-oxygen octahedral chains which are interconnected by double chains of ordered SiO_4 and AlO_4 tetrahedra. In mullite, the AlO_4-SiO_4-sequence is almost random [2] and there exists a certain amount of structural oxygen vacancies. The composition of mullite can be expressed as $Al_2^{VI}(Al_{2+2x}^{IV}Si_{2-2x})O_{10-x}$ where x indicates the amount of missing oxygen with respect to sillimanite and VI and IV indicate sixfold (octahedral) and fourfold (tetrahedral) coordination of aluminium ions. Silicon ions occupy tetrahedral sites only.

Sintering, grain growth, creep and all types of reconstructive reaction processes are strongly controlled by atomic diffusion. Therefore, the diffusivities of oxygen and silicon in single crystalline 2/1-mullite have been carefully determined in previous work using the rare natural isotopes ^{18}O and ^{30}Si as tracer isotopes [3], [4]. Secondary Ion Mass Spectrometry (SIMS) was applied to analyse the depth distribution of the tracer isotopes after the diffusion annealing. Recently, we applied the SIMS technique also to measure the diffusivity of aluminium in single crystalline 2/1-mullite using the pseudo-stable isotope ^{26}Al [5] so that we can now present a complete set of tracer diffusivity data (^{18}O, ^{30}Si, ^{26}Al) of all components of the mullite structure. Based on the results of these tracer diffusivity studies a reaction model for the diffusion controlled mullite formation is discussed in the following.

2. Experimental data

For all tracer diffusion experiments single crystalline 2/1 mullite disks (≈ 1 mm thick) cut perpendicular to [010] and [001] were used to measure the tracer diffusivities along the crystallographic b and c axes. The single crystals were synthesized by Dr. W. Walraffen (Univ. Bonn, Germany) using the Czochralski technique. Details of the crystal growth procedure were published by Guse and Mateika [6].

The b and c axes are very different from a crystallographic point of view, because the mullite structure consists of chains of edge-sharing AlO_6 octahedra running parallel to the crystallographic c axis. These AlO_6 chains are cross-linked by (Al, Si)O_4 tetrahedra forming

double chains, which also run parallel to c [1]. Therefore, a pronounced anisotropy of the diffusivities of the constituents could not be excluded a priori. However, all experimental tracer diffusivity data display virtually no orientation-dependent variation. The slight difference between b and c axes falls into the estimated error range of ± 30 % of diffusion data gained by the method of SIMS depth profiling. Therefore, all evaluated Arrhenius relations represent average values deduced from the diffusivity measurements along the two axes. Since structural arrangements along the a and b axes are very similar in mullite, tracer diffusivities parallel to both directions should also be in a comparable range. So it may be justified to consider tracer diffusivities of the components to be isotropic in mullite.

- Oxygen tracer diffusion

Oxygen diffusion is well studied in many oxides because it can be measured relatively simply by gas/solid exchange experiments [7]. We performed ^{18}O isotope exchange experiments on single crystalline 2/1-mullite samples [3] and obtained the following Arrhenius relation:

$$D_{18O}^{2/1} = (3.71\,^{+13}_{-3}) \times 10^{-5}\,\frac{m^2}{s}\exp\left(-\frac{(433 \pm 21)\,kJ/mol}{RT}\right) \quad (1)$$

In 3/2-mullite, Ikuma et al. [8] evaluated the ^{18}O tracer diffusivity indirectly on micrometer size single crystals by measuring the concentration of $^{18}O_2$ in the gas phase:

$$D_{18O}^{3/2} = (1.32 \pm 0.39) \times 10^{-6}\,\frac{m^2}{s}\exp\left(-\frac{(397 \pm 45)\,kJ/mol}{RT}\right) \quad (2)$$

- Silicon tracer diffusion

In contrast to oxygen, the measurement of silicon diffusivities in oxides is much more difficult. The complications arise from the fact that the natural tracer isotope ^{30}Si has a relatively high natural abundance of about 3.1 %. This circumstance limits the useful diffusion length and requires a deposition technique that allows to prepare very smooth ^{30}Si containing layers on the surface of the specimen. A detailed description of the experimental procedure is given in [4]. The following Arrhenius relation was obtained for the diffusivity of ^{30}Si in single crystalline 2/1-mullite:

$$D_{30Si}^{2/1} = (7.3\,^{+108}_{-6.8}) \times 10^{-2}\,\frac{m^2}{s}\exp\left(-\frac{(612 \pm 39)kJ/mol}{RT}\right) \quad (3)$$

- Aluminium tracer diffusion

Aluminium has no natural tracer isotopes and there are only a few aluminium diffusion data in the literature measured by means of the radiotracer isotope ^{26}Al [9]-[13]. The reason is that

two difficulties are encountered with this radiotracer. Firstly, ^{26}Al is artificial and causes very high production costs, and secondly, it has a half-life time of 7.4×10^5 years with a very low specific activity which makes it difficult to apply classical radiotracer methods [12]. The application of SIMS avoids the problems related to the radioactivity measurement, reduces the necessary amount of ^{26}Al per experiment considerably, and yields a much higher spatial resolution. A detailed description of the measurement of the ^{26}Al diffusivity in 2/1- mullite by means of the SIMS technique is given in [5]. For the diffusivity of ^{26}Al in single crystalline 2/1-mullite we obtained the following Arrhenius relation:

$$D^{2/1}_{26Al} = (9.2\ ^{+92}_{-8.4})\times10^{-3}\ \frac{m^2}{s}\exp\left(-\frac{(517\pm33)kJ/mol}{RT}\right) \quad (4)$$

[*Insert Fig. 1 about here*]

Fig. 1 shows our measured tracer diffusivities (^{18}O, ^{26}Al, ^{30}Si) in single crystalline 2/1-mullite and the ^{18}O diffusivity in single crystalline 3/2-mullite measured by Ikuma et al. [8]. There is only a small difference between the ^{18}O diffusivity in 2/1-mullite and 3/2-mullite. One observes that the diffusivity of ^{30}Si is much lower than the diffusivity of ^{18}O and ^{26}Al. Jaoul et al. [14] and Andersson et al. [15] measured ^{30}Si diffusivities in single crystalline forsterite Mg_2SiO_4 along three crystallographic directions. Both observed that in this silicate, too, silicon diffuses more slowly than oxygen and found no significant anisotropy of the diffusion coefficients. It is assumed that the strong covalent bond within the SiO_4 tetrahedron is an explanation for the low diffusivity of silicon. Furthermore, one observes from Fig. 1 that the diffusivity of ^{26}Al is comparable to the diffusivity of ^{18}O. Le Gall et al. [12] reported a similar result for the diffusivities of ^{26}Al and ^{18}O in single crystalline α-Al_2O_3.

The solid points in Fig. 1 at higher temperatures are experimental data of the parabolic growth constant, k, of diffusion-controlled mullite formation, intensively investigated by Aksay et. al [16], [17]. The quoted authors used diffusion couples made from sapphire and aluminium-silicate glasses of 10.9, 22.8, and 42.2 wt % Al_2O_3. These binary glasses are in equilibrium with mullite at 1678°C, 1753°C, and 1813°C. Thus, sapphire-glass diffusion couples of these compositions at the corresponding annealing temperatures could be used to study the growth kinetics of mullite as an intermediate phase without solution of mullite in the liquid glass

phase. The thickness of the mullite layer increased linearly with the square root of time, indicating that the growth mechanism is diffusion-controlled. The results of Aksay's experiments are outlined in Table 1.

[*Insert Table 1 about here*]

The dashed lines in Fig. 1 are extrapolated tracer diffusivity data from lower temperatures. This means, we know the tracer diffusivities of all components of mullite and the question arises how the measured parabolic growth constants are related to our measured tracer diffusivities. To answer this interesting question we will propose a reaction model for the diffusion-controlled mullite formation in the next chapter.

3. Reaction model

Sung [18] proposed a diffusion-controlled reaction model which is based on the assumption that the oxygen mobility is much lower than the mobility of the cations in mullite. Our tracer diffusion experiments show, however, that silicon is the slowest species compared to oxygen and aluminium in single crystalline 2/1-mullite. This is most probably also valid for 3/2-mullite (s. [8] for the diffusivity of ^{18}O in 3/2-mullite, which is virtually identical to the oxygen diffusivity in 2/1-mullite, as shown in Fig. 1). We will use our experimental observation to derive a more realistic reaction model which is schematically represented in Fig. 2.

[*Insert Fig. 2 about here*]

Because of the low silicon tracer diffusivity we neglect Si^{4+} ion fluxes and consider a formation mechanism where Al_2O_3 is transported by Al^{3+} and O^{2-} ion fluxes through the mullite layer. The fluxes are described by a coordinate system which is fixed to the phase boundary I. Such a coordinate system becomes applicable when one cation has a much lower mobility than other species [19]. The intrinsic drift velocity, $d\xi/dt$, describes the drift velocity of phase boundary II relative to phase boundary I. A simple, but fundamental, relation between the Al^{3+} and O^{2-} fluxes in Fig. 2 is given in the absence of space charges

$$3\,j_{Al^{3+}} - 2\,j_{O^{2-}} = 0 \tag{5}$$

In the literature (p. 229 in [20]) one finds the concept of a molecular flux, $j_{A_\alpha B_\beta}$, and a molecular diffusion coefficient, $D_{A_\alpha B_\beta}$, which is used to express the fact that the process takes places as if an entity $A_\alpha B_\beta$ of fixed composition (a "molecule" or better a "formula unit") were migrating. The condition for a molecular flux of Al_2O_3 is

$$j_{Al_2O_3} = \frac{j_{Al^{3+}}}{2} = \frac{j_{O^{2-}}}{3} \tag{6}$$

where j_i is the flux of the ion i (Al^{3+}, O^{2-}). Equation (6) ensures the composition to remain constant and is identical to equation (5) which excludes any build-up of space charge. That is, one can describe the two coupled Al^{3+} and O^{2-} ion fluxes by a single molecular flux of Al_2O_3

$$j_{Al_2O_3} = -\frac{c_{Al_2O_3} D_{Al_2O_3}}{RT} \frac{d\mu_{Al_2O_3}}{dx} \tag{7}$$

were c is the molecular concentration, D the molecular (ambipolar) diffusion coefficient and μ the molecular chemical potential of Al_2O_3 in the solid mullite layer. In ceramics the term ambipolar diffusion coefficient is preferred as it implies the fact of the migration of coupled charges (p. 232 in [20] or p. 238 in [21]). For the ambipolar diffusion coefficient of Al_2O_3 in equation (7) one gets after a lengthy calculation (see appendix A.1)

$$\frac{1}{D_{Al_2O_3}} = \frac{2}{D_{Al^{3+}}} + \frac{3}{D_{O^{2-}}} \tag{8}$$

where D_i is the diffusion coefficient of the ion i (Al^{3+}, O^{2-}) which is related to the random thermal motion of the ions. In diffusional transport the random thermal motion is superposed on a drift resulting from field forces like the gradient of the chemical potential. Using equation (7) one gets for the average drift velocity of Al_2O_3

$$v_{Al_2O_3} = \frac{j_{Al_2O_3}}{c_{Al_2O_3}} = -\frac{D_{Al_2O_3}}{RT} \frac{d\mu_{Al_2O_3}}{dx} \tag{9}$$

Since the forces ($d\mu_{Al_2O_3}/dx = 2\,d\mu_{Al^{3+}}/dx + 3\,d\mu_{O^{2-}}/dx$) are small on the atomic length scale, diffusion coefficients established under equilibrium conditions (i.e., vanishing forces) can be used to describe the drift of the ions (p. 107 in [22]).

The relation of the self diffusion coefficients, D_i, of the ions in equation (8) to our measured tracer diffusivities, D_{*i}, is given by $D_{*i} = f_{*i} D_i$, where f_{*i} is the so-called correlation factor (p. 97 in [20]). Correlation factors for self diffusion are calculated for different diffusion mechanisms and crystal structures and are often in the order of 1 (p. 98 in [20]). Therefore, we can calculate the ambipolar diffusion coefficient of Al_2O_3 in a first order approximation by our measured tracer diffusivities

$$\frac{1}{D_{Al_2O_3}} = \frac{2 f_{^{26}Al}}{D_{^{26}Al}} + \frac{3 f_{^{18}O}}{D_{^{18}O}} \cong \frac{2}{D_{^{26}Al}} + \frac{3}{D_{^{18}O}} \qquad (10)$$

Correlation effects diminish the effectiveness of atomic jumps ($f_{*i} \leq 1$) in diffusional random motion (p. 110 in [22]), that is, ambipolar diffusion coefficients calculated by our tracer diffusivities are lower limits.

To calculate the parabolic growth constant, k, it is assumed that the ion fluxes are quasi-steady which means that during a specific time interval the fluxes can be considered to be constant in space. Because the concentration of Al_2O_3 is practically constant inside the mullite layer the drift velocity of Al_2O_3 is also practically independent of x. Separating variables and integrating equation (9) between the phase boundaries I and II results in (p. 168 in [22])

$$v_{Al_2O_3} \xi = -\frac{1}{RT} \int_{(I)}^{(II)} D_{Al_2O_3} d\mu_{Al_2O_3} \qquad (11)$$

where ξ is the thickness of the mullite layer. The drift velocity of phase boundary II relative to phase boundary I is equal to the average drift velocity of the Al_2O_3 molecules, $d\xi/dt = v_{Al_2O_3}$, so that one calculates the parabolic growth constant, k, by separating variables and integrating equation (11)

$$k = \frac{\xi^2}{2t} = -\frac{1}{RT} \int_{(I)}^{(II)} D_{Al_2O_3} d\mu_{Al_2O_3} \qquad (12)$$

To integrate the right hand side of equation (12) we must know the dependence of the ambipolar diffusion coefficient on the chemical potential which requires the application of an appropriate defect model.

Aksay et al. [17] used diffusion couples with sapphire and aluminium-silicate glasses at different temperatures. For every temperature, the Al_2O_3 concentration of the binary glass was chosen so that the glass phase was in equilibrium with the mullite phase. That is, any growth of the mullite layer requires Al_2O_3 to be transported through the mullite layer from the

sapphire sample side. This transport is enabled by a flux of freely migrating defects which are formed during the mullite formation reaction. We assume that during the reaction of "SiO_2" from the binary glass with "Al_2O_3", which is located on regular sites in the mullite structure, aluminium vacancies and oxygen vacancies are formed according to the following reaction (applying the Kröger-Vink notation)

$$2\,SiO_2 + 6\,Al_{Al}^{\times} + 9\,O_O^{\times} = 6\,V_{Al}''' + 9\,V_O^{\bullet\bullet} + Al_6Si_2O_{13} \qquad (13)$$

where $Al_6Si_2O_{13}$ is 3/2-mullite. If local defect equilibrium is assumed one gets from equation (13) the defect equilibrium constant

$$K_d = \frac{a_{V_{Al}'''}^{6}\, a_{V_O^{\bullet\bullet}}^{9}}{a_{SiO_2}^{2}} \qquad (14)$$

where a_i is the activity of the species i (SiO_2, aluminium vacancies, oxygen vacancies). Furthermore, we assume that the dilution of the vacancies is sufficient to express activities by concentrations, $a_V \cong [V]$. Using the condition for electroneutrality, $3[V_{Al}'''] = 2[V_O^{\bullet\bullet}]$, one gets from equation (14) a dependence of the vacancy concentration from the SiO_2 activity

$$[V_{Al}'''] = \alpha\, a_{SiO_2}^{2/15} \quad \text{and} \quad [V_O^{\bullet\bullet}] = \frac{3}{2}\alpha\, a_{SiO_2}^{2/15} \quad \text{with} \quad \alpha \equiv \left(\frac{2}{3}\right)^{-3/5} K_d^{1/15} \qquad (15)$$

If the diffusivity of aluminium ions is proportional to the concentration of aluminium vacancies, $D_{Al^{3+}} \propto [V_{Al}''']$, and if the diffusivity of oxygen ions is proportional to the concentration of oxygen vacancies, $D_{O^{2-}} \propto [V_O^{\bullet\bullet}]$, one can conclude from equations (8) and (15) that the ambipolar diffusion coefficient of Al_2O_3 is proportional to $a_{SiO_2}^{2/15}$

$$D_{Al_2O_3} = D_{Al_2O_3}^{I} \left(\frac{a_{SiO_2}}{a_{SiO_2}^{I}} \right)^{2/15} \qquad (16)$$

where the superscript I denotes values at the phase boundary I. Inserting equation (16) into equation (12) gives after some calculations (see appendix A.2)

$$k = n\,(D_{Al_2O_3}^{II} - D_{Al_2O_3}^{I}) \quad \text{with} \quad n = 5 \qquad (17)$$

where the superscripts I and II denote values of the ambipolar diffusion coefficient at the corresponding phase boundaries in Fig. 2.

4. Discussion

The calculations in chapter 3 show that the parabolic growth constant, k, is proportional to the difference of the ambipolar diffusion coefficients of Al_2O_3 at the phase boundaries (see equation (17)) where the calculated proportional constant, n, depends on the applied defect model and is 5 for the proposed one (equation (13)). It is interesting to note that only the difference of the absolute values of the ambipolar diffusion coefficients plays a role for the diffusion controlled growth kinetics of the reaction layer (mullite). The absolute values of the ambipolar diffusion coefficients of Al_2O_3 at both phase boundaries are determined by the freely migrating defects which are formed during the mullite formation reaction. Equation (17) would be the most direct way to calculate parabolic growth constants from diffusivity data. However, this procedure requires the same defect chemistry to be valid for the entire composition range of mullite and it requires the measurements of the two diffusion constants.

Because diffusivity measurements are often only possible at one of the two interfaces it is useful to express equation (17) by

$$k = D^{I}_{Al_2O_3} \Delta R \tag{18}$$

with the dimensionless factor

$$\Delta R = n \frac{D^{II}_{Al_2O_3} - D^{I}_{Al_2O_3}}{D^{I}_{Al_2O_3}} \tag{19}$$

where we have assumed that the ambipolar diffusion coefficient of Al_2O_3 at phase boundary I corresponds to our calculated ambipolar diffusion coefficient of Al_2O_3 from the measured tracer diffusivity data. The disadvantage of this notation is that it seems to suggest that $D^{I}_{Al_2O_3}$ and the dimensionless factor, ΔR, are independent terms, with the wrong implication that k is proportional to the absolute value of $D^{I}_{Al_2O_3}$. The advantage of this notation will, however, become obvious in the development given below.

The diffusivities at the interfaces are proportional to the freely migrating defects at the interfaces so that one gets for the dimensionless factor ΔR (considering equations (15) and (16))

$$\Delta R = n \frac{[V'''_{Al}]^{II} - [V'''_{Al}]^{I}}{[V'''_{Al}]^{I}} = n \frac{[V^{\bullet\bullet}_{O}]^{II} - [V^{\bullet\bullet}_{O}]^{I}}{[V^{\bullet\bullet}_{O}]^{I}} \tag{20}$$

As ΔR is proportional to the relative change of the concentrations of the transporting defects it

can be calculated from our proposed defect model (see appendix A.3)

$$\Delta R = 5\left[(a^{II}_{SiO_2})^{\frac{2}{15}} \exp\left(-\frac{\Delta_r G^{\circ}_{Al_6Si_2O_{13}}}{15\,RT}\right) - 1\right] \tag{21}$$

where $\Delta_r G^{\circ}_{Al_6Si_2O_{13}}$ is the Gibbs free energy for the formation of 3/2-mullite from the parent oxides and $a^{II}_{SiO_2}$ is the activity of SiO_2 in the aluminium-silicate melt at phase boundary II.

In the absence of any plausible defect model one could assume, as a first approximation, a constant diffusion coefficient, $D_{Al_2O_3} = D^{I}_{Al_2O_3} = D^{II}_{Al_2O_3}$, which allows the simplest integration of the right hand side of equation (12). This gives

$$k_0 = D^{I}_{Al_2O_3}\,\Delta R_0 \tag{22}$$

with the dimensionless factor ΔR_0

$$\Delta R_0 = \frac{\left|\Delta\mu_{Al_2O_3}\right|}{RT} \quad \text{and} \quad \Delta\mu_{Al_2O_3} = \mu^{II}_{Al_2O_3} - \mu^{I}_{Al_2O_3} \tag{23}$$

where the superscripts I and II denote values of the chemical potential of Al_2O_3 at the corresponding phase boundaries in Fig. 2 and the subscript 0 indicates values of a first approximation. The difference of the chemical potential of Al_2O_3 at both phase boundaries can be calculated by means of the Gibbs free energy of formation of 3/2-mullite from the oxides and the activity of SiO_2 in the aluminium-silicate melt at phase boundary II (see appendix A.4).

$$\Delta\mu_{Al_2O_3} = \frac{\Delta_r G^{\circ}_{Al_6Si_2O_{13}}}{3} - \frac{2}{3}RT\ln(a^{II}_{SiO_2}) \tag{24}$$

[*Insert Table 2 about here*]

The dimensionless factors ΔR_0 and ΔR for the 3/2-mullite formation from the oxides are calculated in Table 2 for experimental temperatures used by Aksay et. al [17] (see Table 1). It is obvious that both factors are practically equal in this temperature range. Comparing equations (18) and (22) through the ratio

$$\frac{k}{k_0}=\frac{\Delta R}{\Delta R_0}=\frac{5\left[\left(a_{SiO_2}^{(II)}\right)^{\frac{2}{15}}\exp\left(-\frac{\Delta_r G^{\circ}_{Al_6Si_2O_{13}}}{15\,RT}\right)-1\right]}{-\frac{\Delta_r G^{\circ}_{Al_6Si_2O_{13}}}{3\,RT}+\frac{2}{3}\ln(a_{SiO_2}^{(II)})} \qquad (25)$$

one can conclude that the reason for this observation is the low value of the Gibbs free energy, $\Delta_r G^{\circ}_{Al_6Si_2O_{13}} \approx -35\,kJ/mol$, for the formation of 3/2-mullite from the oxides and the high experimental temperatures, $RT \approx 17\,kJ/mol$. Therefore, our proposed defect model does practically not improve the agreement between the experimental data and the calculated parabolic growth rates in this temperature range, so that it is not meaningful to try a quantitatively validation of this model. It is, however, extremely useful to discuss this phenomenon from a more general point of view. The derivation of the factor of first approximation, ΔR_0, starts with the assumption that the (chemical) diffusion coefficient, D, in the reaction layer is practically constant and we assume, of course, that the calculated parabolic growth rate is practically correct, which implies the approximate relation

$$\frac{\Delta R_0}{n}\approx\frac{\Delta R}{n} \quad \text{if} \quad D\approx \text{constant} \qquad (26)$$

where n is a correct number evaluated from a correct defect model. Considering equations (23) and (19) we can express relation (26) by

$$\left|\frac{\Delta\mu_i}{n\,RT}\right|\approx\left|\frac{D_i^{II}-D_i^{I}}{D_i^{I}}\right| \quad \text{if} \quad D\approx \text{constant} \qquad (27)$$

where $i = Al_2O_3$ for the proposed mullite formation reaction. Such a relation holds for all formation reactions which can be treated mathematically in the same formal manner.

The right hand side of relation (27) corresponds to the relative change of the diffusivity across the mullite layer. That is, the assumption that the diffusion coefficient in the reaction layer is practically constant is fulfilled if $|\Delta\mu_i| < |n|\,RT$. This case is generally more likely at higher temperatures and reactions with low Gibbs free energy of formation (e.g the considered mullite formation from the oxides). One has then $\Delta R_0 \approx \Delta R$ and can calculate the parabolic growth constant by the simple equation (22). The application of a defect model does practically not improve the calculated parabolic growth constants in the considered temperature range so that it becomes difficult to prove a proposed defect model quantitatively from experimentally determined parabolic growth constants.

The case $|\Delta\mu_i| > |n|RT$ is clearly in conflict with relation (27) which is based on the assumption that the diffusion coefficient in the reaction layer is approximately constant. This case is generally more likely at lower temperatures and reactions with high Gibbs free energy of formation. It is then not reasonable to assume a constant diffusion coefficient to integrate equation (12), so that an appropriate defect model is necessary to calculate parabolic growth constants.

The measured parabolic growth rates of 3/2-mullite are by a factor of 4 to 17 larger (see the ratio k_{exp}/k_{calc} in Table 2) than the parabolic growth rates calculated from our measured tracer diffusivities in single crystalline 2/1-mullite. Two terms were used to calculate the theoretical parabolic growth rates (see equation (18)): a diffusivity term and a dimensionless term, the factor, ΔR, which could be expressed in a good approximation by the normalised change of the chemical potential of Al_2O_3, $|\Delta\mu_{Al_2O_3}|/RT$, across the reaction layer. Hence, a strong deviation from the experimental values cannot be explained by a wrong calculation of the factor, ΔR, because this would imply a very erroneous calculation of the chemical potential of Al_2O_3. The observed deviation from the experimental values must be induced by the calculation of the diffusivity term in equation (18). This term was calculated by equation (10) using our measured bulk tracer diffusivities. As we mentioned above the use of tracer diffusivities, and neglecting correlation effects, will result principally in a lower limit value of the diffusivity term in equation (18). Furthermore, grain boundary diffusion has to be considered to explain why the diffusivities of the oxygen ions and the aluminium ions during the mullite formation are significantly higher than our measured bulk tracer diffusivities.

Grain boundary tracer diffusivities of mullite are known for the ^{18}O isotope only [23]. In the grain boundaries a much higher ^{18}O diffusivity (up to a factor of 10^4) was observed than in the bulk. The amount of Al_2O_3 which is transported through the grain boundaries is proportional to the volume fraction of grain boundaries in the mullite layer. Therefore, an effective diffusion coefficient can be calculated by the Hart-Mortlock equation [24][25]

$$D_{eff} = s\,g\,D_{gb} + (1 - s\,g)\,D \qquad (28)$$

where D is the bulk diffusivity, D_{gb} the grain boundary diffusivity, g the volume fraction of grain boundaries, and s the grain boundary segregation factor ($s = 1$ for self-diffusion). Assuming a similar enhancement (a factor of 10^4) of the ^{26}Al diffusivities in the grain boundaries one can conclude from the Hart-Mortlock equation that volume fractions of grain boundaries from 2.9×10^{-4} to 1.6×10^{-3} are sufficient to explain the observed discrepancies

between calculated and measured parabolic growth rates. For a cubic grain geometry one can estimate the grain size, d, by $d \approx 3\delta / g$ (p. 206 in [26]). Assuming an average grain boundary width δ = 1 nm one gets corresponding cubic grain sizes from 10 µm to 2 µm.

This explanation is plausible, however, the larger discrepancy at higher temperatures is somewhat contradictory to conventional thinking about grain boundary effects (i.e., the relative contribution from grain boundary diffusion is often larger at lower temperatures). Another explanation could be impurity effects on diffusion, even with relatively pure starting materials. For example, one observes a scatter band of about one order of magnitude for measured oxygen diffusivities in nominally undoped α-Al_2O_3 which is mainly explained by impurities which induce extrinsic point defects and affect the diffusion process [27]. Furthermore, we have assumed that the influence of the Si/Al ratio does not strongly affect the diffusion process. This assumption is based on the low value of the Gibbs free energy of formation of mullite and on the resulting close agreement of the oxygen diffusivity data obtained for (single crystalline) 2/1-mullite and 3/2-mullite (see also [28] for further discussion) but is open to debate for the aluminium diffusivity.

This discussion shows that the parabolic growth rates calculated from our measured bulk tracer diffusivity data of oxygen and aluminium define at least a lower limit of the experimentally observed growth rates. With the exception of the mullite formation data set at the highest temperature (1813 °C) the discrepancy between parabolic rate constants calculated on the basis of (extrapolated) bulk diffusion data and the experimentally determined rate constants is about half an order of magnitude, which clearly supports our model, taking into account that the details of the growth experiment (impurity concentrations etc.) are not fully evident from the literature.

5. Summary

An essential result of our tracer diffusivity studies in single crystalline 2/1-mullite is the very low diffusivity of ^{30}Si compared to the diffusivities of ^{26}Al and ^{18}O, which are almost equal. Based on this observation we propose a diffusion-controlled mullite formation model which assumes that the growth kinetics of a mullite layer is controlled by the diffusion of aluminium ions and oxygen ions. The two ionic fluxes can be described by a single molecular (ambipolar) flux of Al_2O_3 which transports Al_2O_3 through the mullite layer and reacts with SiO_2 to mullite. The ambipolar flux of Al_2O_3 is enabled by freely migrating defects which are

formed during the mullite formation reaction.

The reaction of SiO_2 with Al_2O_3 on regular sites in the mullite structure requires the formation of aluminium vacancies and oxygen vacancies (equation (13)). Based on this defect model we derive equation (17) to calculate the parabolic growth constant of mullite formation. However, the direct application of this equation requires the proposed defect model to be valid in the whole mullite layer and necessitates the measurement of tracer diffusivities at the two interfaces. Therefore, we write equation (17) into the form of equation (18) by the definition of a dimensionless factor, ΔR, and assume that the ambipolar diffusion coefficient of Al_2O_3 at interface I corresponds to the ambipolar diffusion coefficient of Al_2O_3 calculated from our tracer diffusivity data. The factor, ΔR, is then calculated by means of the proposed defect model (see equation (21)).

Further, it is demonstrated that because of the fairly low value of the Gibbs free energy of formation of mullite the ambipolar diffusion coefficient of Al_2O_3 in the mullite layer is practically constant.

To calculate the parabolic growth rate of mullite formation we need the ambipolar diffusion coefficient of Al_2O_3 in the mullite layer which can principally be calculated from the diffusion coefficients of aluminium and oxygen (equation (8)). Neglecting correlation effects we calculate the ambipolar diffusion coefficient of Al_2O_3 from our measured tracer diffusivity data (equation (10)). The results of this calculation are compiled in Table 2 and show that our calculated values are about a factor of 5 lower than the measured values by Aksay et al. [17], at least below 1750 °C. Taking into account typical experimental errors in layer growth experiments this fairly small discrepancy supports our reaction model. Our calculated values thus define a lower limit of the parabolic growth rate.

Acknowledgement

Financial support from Deutsche Forschungsgemeinschaft (DFG) is gratefully acknowledged. The comments of an anonymous reviewer helped to improve the manuscript.

Appendix A

For the following derivations it is assumed that local thermodynamical equilibrium is maintained within the reaction layer and also at the phase boundaries I and II, so that the following equilibrium condition is valid

$$2\,Al^{3+} + 3O^{2-} = Al_2O_3 \tag{29}$$

$$2\,\eta_{Al^{3+}} + 3\eta_{O^{2-}} = \mu_{Al_2O_3} \tag{30}$$

where η is the electrochemical potential of electrically charged particles (Al^{3+}, O^{2-}) and μ is the chemical potential of the uncharged particle (Al_2O_3). The chemical reaction equation of the 3/2-mullite formation from the oxides is given by

$$2\,SiO_2 + 3\,Al_2O_3 = Al_6Si_2O_{13} \tag{31}$$

The reaction equilibrium constant, K_r, can be written as

$$K_r = \frac{a_{Al_6Si_2O_{13}}}{a^3_{Al_2O_3}\,a^2_{SiO_2}} = \exp\left(-\frac{\Delta_r G^\circ_{Al_6Si_2O_{13}}}{RT}\right) \tag{32}$$

where a_i is the activity of component i ($Al_6Si_2O_{13}$, Al_2O_3, SiO_2) and $\Delta_r G^\circ_{Al_6Si_2O_{13}}$ is the Gibbs free energy of formation of 3/2-mullite from the oxides which can be calculated by the free energy of the formation from elements, $\Delta_f G^\circ_i$ tabulated in [29] or [30],

$$\Delta_r G^\circ_{Al_6Si_2O_{13}} = \Delta_f G^\circ_{Al_6Si_2O_{13}} - 3\Delta_f G^\circ_{Al_2O_3} - 2\Delta_f G^\circ_{SiO_2} \tag{33}$$

The activity of 3/2-mullite is 1 in the mullite layer so that equation (32) yields

$$2\,RT\ln\left(a_{SiO_2}\right) + 3\,RT\ln\left(a_{Al_2O_3}\right) = \Delta_r G^\circ_{Al_6Si_2O_{13}} \tag{34}$$

A.1 Derivation of equation (8)

The fluxes of aluminium and oxygen ions are given by

$$j_{Al^{3+}} = -\frac{c_{Al^{3+}}\,D_{Al^{3+}}}{RT}\frac{d\eta_{Al^{3+}}}{dx}$$

$$j_{O^{2-}} = -\frac{c_{O^{2-}}\,D_{O^{2-}}}{RT}\frac{d\eta_{O^{2-}}}{dx} \tag{35}$$

where c_i, D_i and η_i are the concentration, the diffusion coefficient and the electrochemical

potential of the ion i (Al^{3+}, O^{2-}), respectively [31]. The gradient of the electrochemical potentials can be expressed by

$$\frac{d\eta_{Al^{3+}}}{dx} = \frac{d\mu_{Al^{3+}}}{dx} + 3F\frac{d\varphi}{dx}$$
$$\frac{d\eta_{O^{2-}}}{dx} = \frac{d\mu_{O^{2-}}}{dx} - 2F\frac{d\varphi}{dx} \qquad (36)$$

where F is the Faraday constant and φ the electrical potential. The condition for electroneutrality, equation (5), is used to eliminate the unknown term F×dφ/dx from the flux equations.

$$F\frac{d\varphi}{dx} = -\frac{3c_{Al^{3+}}D_{Al^{3+}}\frac{d\mu_{Al^{3+}}}{dx} - 2c_{O^{2-}}D_{O^{2-}}\frac{d\mu_{O^{2-}}}{dx}}{9c_{Al^{3+}}D_{Al^{3+}} + 4c_{O^{2-}}D_{O^{2-}}} \qquad (37)$$

Inserting equation (37) into the flux equations (35)-(36) and respecting equation (5) and (30) one gets for the ion fluxes

$$\frac{j_{Al^{3+}}}{2} = \frac{j_{O^{2-}}}{3} = -\frac{\langle cD\rangle_{Al_2O_3}}{RT}\frac{d\mu_{Al_2O_3}}{dx} \qquad (38)$$

with the shortcut

$$\langle cD\rangle_{Al_2O_3} \equiv \frac{c_{Al^{3+}}D_{Al^{3+}} \times c_{O^{2-}}D_{O^{2-}}}{9c_{Al^{3+}}D_{Al^{3+}} + 4c_{O^{2-}}D_{O^{2-}}} \qquad (39)$$

By equation (7) an ambipolar diffusion coefficient was defined. Comparing equations (6), (7) and (38) one concludes that the ambipolar diffusion coefficient is given by

$$D_{Al_2O_3} = \frac{\langle cD\rangle_{Al_2O_3}}{c_{Al_2O_3}} = \frac{D_{Al^{3+}}D_{O^{2-}}}{9(c_{Al_2O_3}/c_{O^{2-}})D_{Al^{3+}} + 4(c_{Al_2O_3}/c_{Al^{3+}})D_{O^{2-}}} \qquad (40)$$

and finally because of the concentration relations

$$c_{Al_2O_3} = \frac{c_{Al^{3+}}}{2} = \frac{c_{O^{2-}}}{3} \qquad (41)$$

one derives equation (8). Considering equation (6) and equation (41) one concludes

$$v = \frac{j_{Al_2O_3}}{c_{Al_2O_3}} = \frac{j_{Al^{3+}}}{c_{Al^{3+}}} = \frac{j_{O^{2-}}}{c_{O^{2-}}} \qquad (42)$$

Thus, all particles (Al_2O_3, Al^{3+}, O^{2-}) considered in the proposed mullite formation model migrate with the same drift velocity, v.

A.2 Derivation of equation (17)

By definition the chemical potential of Al_2O_3 is given by

$$\mu_{Al_2O_3} = \mu^{\circ}_{Al_2O_3} + RT \ln(a_{Al_2O_3}) \tag{43}$$

considering also equation (34) one can express equation (12) by

$$k = \frac{2}{3}\int_{(I)}^{(II)} D_{Al_2O_3}\, d\ln(a_{SiO_2}) = \frac{2}{3}\int_{(I)}^{(II)} \frac{D_{Al_2O_3}}{a_{SiO_2}}\, da_{SiO_2} \tag{44}$$

Inserting equation (16) gives

$$k = 5\frac{D^{I}_{Al_2O_3}}{(a^{I}_{SiO_2})^{2/15}}\left[(a^{II}_{SiO_2})^{2/15} - (a^{I}_{SiO_2})^{2/15}\right] = 5(D^{II}_{Al_2O_3} - D^{I}_{Al_2O_3}) \tag{45}$$

A.3 Derivation of equation (21)

The factor ΔR is defined by equation (18). Considering equations (45) and (16) gives

$$\Delta R = 5\left[\frac{(a^{II}_{SiO_2})^{2/15}}{(a^{I}_{SiO_2})^{2/15}} - 1\right] \tag{46}$$

At interface I the activity of Al_2O_3 is 1 (see Fig. 2) so that one can calculate the activity of SiO_2 at interface I using equation (34)

$$(a^{I}_{SiO_2})^{2/15} = \exp\left(\frac{\Delta G^{\circ}_{Al_6Si_2O_{13}}}{15\,RT}\right) \tag{47}$$

Inserting equation (47) into equation (46) gives equation (21).

A.4 Derivation of equation (24)

The activity of Al_2O_3 is 1 at interface I and $a^{II}_{Al_2O_3}$ at interface II (see Fig. 2) so that one gets from equation (43) for the difference of the chemical potential

$$\Delta\mu_{Al_2O_3} = \mu^{II}_{Al_2O_3} - \mu^{I}_{Al_2O_3} = RT \ln(a^{II}_{Al_2O_3}) \tag{48}$$

Considering equation (34) one gets equation (24).

References

[1] H. Schneider, K. Okada and J.A. Pask, *Mullite and Mullite Ceramics* (John Wiley & Sons Ltd., Chichester, 1994).

[2] M. Schmücker, K.J.D. MacKenzie, M.E. Smith, D.L. Carroll and H. Schneider, J. Am. Ceram. Soc. **88** 2935 (2005).

[3] P. Fielitz, G. Borchardt, M. Schmücker, H. Schneider, M. Wiedenbeck, D. Rhede, S. Weber and S. Scherrer, J. Am. Ceram. Soc. **84** [12] 2845 (2001).

[4] P. Fielitz, G. Borchardt, M. Schmücker and H. Schneider, Phys. Chem. Chem. Phys. **5** 2279 (2003).

[5] P. Fielitz, G. Borchardt, M. Schmücker and H. Schneider, Solid State Ionics (2006), in press.

[6] W. Guse and D. Mateika, J. Cryst. Growth **22** 237 (1974).

[7] P. Fielitz and G. Borchardt, Solid State Ionics **144** 71 (2001).

[8] Y. Ikuma, E. Shimada, S. Sakano, M. Oishi, M. Yokoyama and Z. Nakagawa, J. Electrochem. Soc. **146** 4672 (1999).

[9] A.E. Paladino and W.D. Kingery, J. Chem. Phys. **37** 957 (1962).

[10] M. Beyeler and Y. Adda, J. Physique **29** 345 (1968).

[11] L.N. Larikov, V.V. Geichenko and V.M. Fal'chenko, *Diffusion Processes in Ordered Alloys* (Amerind Publ. Co, New Delhi, 1981) pp. 111–121.

[12] M. Le Gall, B. Lesage and J. Bernardini, Phil. Mag. A **70** 761 (1994).

[13] G.H. Frischat, J. Am. Ceram. Soc. **52** 625 (1969).

[14] O. Jaoul, M. Poumellec, C. Froidevaux and A. Havette, in *Anelasticity in the Earth*, edited by F.D. Stacey et al. (Geodyn. Ser. Vol. 4, AGU, Washington, DC, 1981) pp. 95–100.

[15] K. Andersson, G. Borchardt, S. Scherrer and S. Weber, Fresenius Z. Anal. Chem. **333** 383 (1989).

[16] I.A. Aksay, Diffusion and Phase Relationship Studies in the Alumina-Silica System. PhD thesis, University of California, Berkeley (1973).

[17] I.A. Aksay and J.A. Pask, J. Am. Ceram. Soc. **58** [11-12] 507 (1975).

[18] Y.-M. Sung, Acta mater. **48** 2157 (2000).

[19] A.R. Cooper Jr. and J.H. Heasley, J. Am. Ceram. Soc. **49** [5] 280 (1966).

[20] J. Philibert, *Atom Movements - Diffusion and Mass Transport in Solids* (Les Éditions de Physique, Les Ulis Cedex A, 1991).

[21] Y.-M. Chiang, D.P. Birnie and W.D. Kingery, *Physical Ceramics: Principles for Ceramic Science and Engineering* (John Wiley & Sons, New York, 1997).

[22] H. Schmalzried, *Chemical Kinetics of Solids* (VCH, Weinheim, 1995).

[23] P. Fielitz, G. Borchardt, M. Schmücker, H. Schneider and P. Willich, J. Am. Ceram. Soc. **87** [12] 2232 (2004).

[24] E.W. Hart, Acta Metall. **5** 597 (1957).

[25] A.J. Mortlock, Acta Metall. **8** 132 (1960).

[26] I. Kaur, Y. Mishin, W. Gust, *Fundamentals of Grain and Interphase Boundary Diffusion* (John Wiley & Sons Ltd., Chichester, 1995).

[27] D. Prot and C. Monty, Phil. Mag. A **73** [4] 899 (1996).

[28] P. Fielitz, G. Borchardt, M. Schmücker and H. Schneider, J. Eur. Ceram. Soc. **21** 2577 (2001).

[29] I. Barin, *Thermochemical Data of Pure Substances* (Part I + II, VCH Publishers, Weinheim, 1989).

[30] M.W. Chase Jr., C.A. Davies, J.R. Downey Jr., D.J. Frurip, R.A. McDonald and A.N. Syverud, *JANAF Thermochemical Tables* (3rd ed., ACS, AIP, NBS, New York, 1986).

[31] H. Schmalzried, *Solid State Reactions* (2^{nd} ed., Verlag Chemie, Weinheim, 1981).

Tables

Table 1 Experimental conditions and data for sapphire-equilibrium-melt runs [17], where t is the annealing time, ξ is the mullite layer thickness, and k_{exp} the experimental parabolic growth constant.

T °C	Melt mol % Al_2O_3	Mullite mol % Al_2O_3	t min	ξ μm	$k_{exp} = \xi^2/(2t)$ m^2/s
1678	6.75	58.6-62.7	12,182	10	6.8×10^{-17}
1678	6.75	58.6-62.7	47,380	18	5.7×10^{-17}
1753	14.9	58.6-62.7	6,608	13	2.1×10^{-16}
1813	30.2	59.9-62.7	10,025	36	1.1×10^{-15}

Table 2 Parabolic growth rates calculated from the measured tracer diffusivities of aluminium and oxygen using equations (10), (18) and (21) (compare with experimental data in Table 1). The activity of SiO_2 at phase boundary II, $a^{II}_{SiO_2}$, was approximated by the molar fraction of SiO_2 in the aluminium-silicate melt. The free energy, $\Delta_r G^\circ_{Al_6Si_2O_{13}}$, for the formation of 3/2-mullite from the oxides was calculated with equation (33) using thermochemical data from [29]. The dimensionless factor of first approximation, ΔR_0, was calculated by equations (23), (24).

T °C	RT kJ/mol	$\Delta_r G^\circ_{Al_6Si_2O_{13}}$ kJ/mol	$a^{II}_{SiO_2}$	ΔR_0	ΔR	$D_{Al_2O_3}$ m^2/s	k_{calc} m^2/s	k_{exp} / k_{calc}
1678	16.2	-33.8	0.93	0.65	0.69	2.1×10^{-17}	1.5×10^{-17}	4.6
1678	16.2	-33.8	0.93	0.65	0.69	2.1×10^{-17}	1.5×10^{-17}	3.9
1753	16.8	-35.3	0.85	0.59	0.63	6.1×10^{-17}	3.8×10^{-17}	5.6
1813	17.3	-36.5	0.70	0.46	0.48	1.3×10^{-16}	6.4×10^{-17}	17

Figure Captions

Fig. 1 Compilation of our measured tracer diffusivities (^{18}O, ^{26}Al, ^{30}Si) in single crystalline 2/1-mullite. Ikuma et al. [8] measured the ^{18}O diffusivity in single crystalline 3/2-mullite. Also shown are data of the parabolic growth constant, k, of mullite formation measured by Aksay et al. [17] via high-temperature diffusion couple experiments.

Fig. 2 Schematic representation of the reaction model for the mullite formation. Al_2O_3 is transported through the solid mullite layer by means of intrinsic Al^{3+} and O^{2-} ion fluxes and reacts to 3/2-mullite with SiO_2 from the aluminosilicate melt which is in equilibrium with mullite. The chemical potential of Al_2O_3 decreases across the mullite layer, the limiting values are $\mu^{I}_{Al_2O_3}$ in α-Al_2O_3 and $\mu^{II}_{Al_2O_3}$ in the aluminosilicate melt.

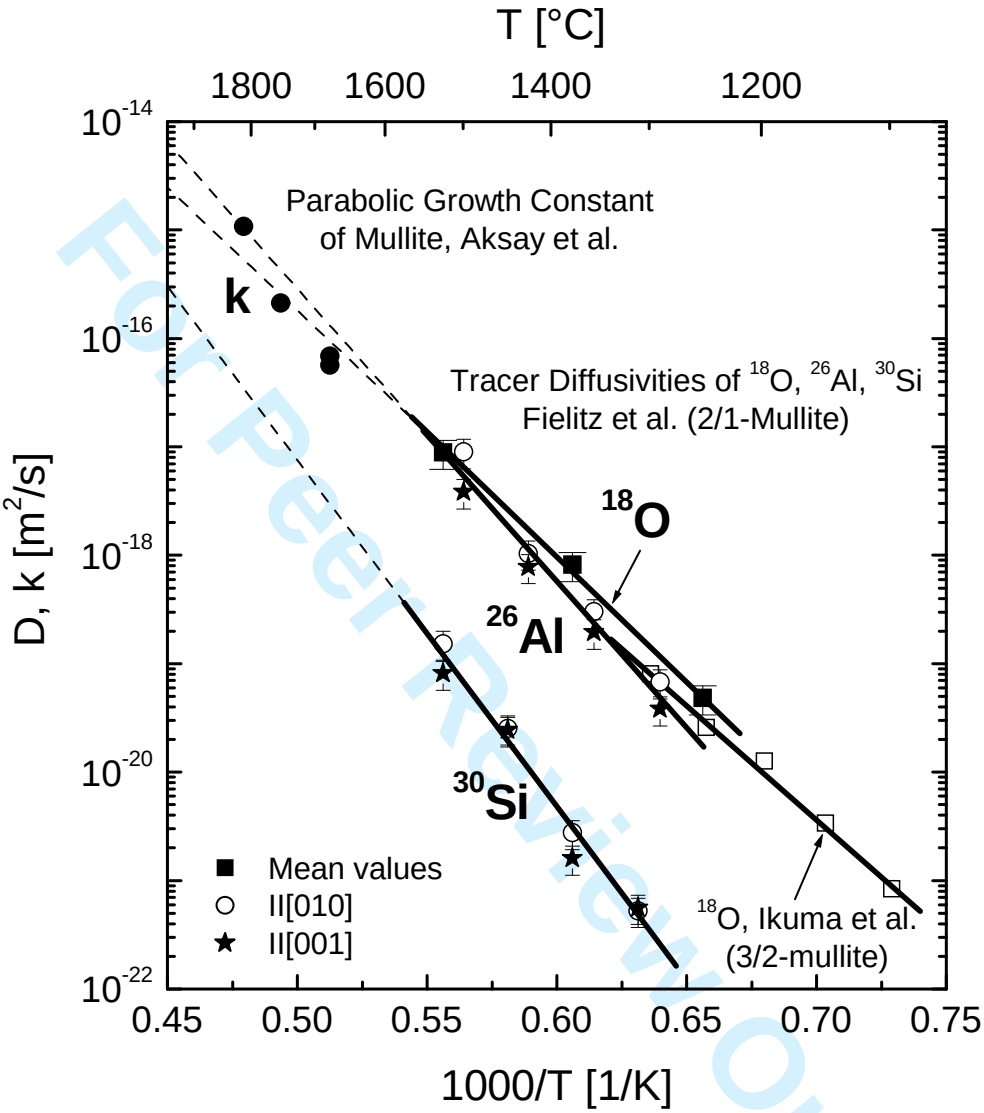

Fig. 1

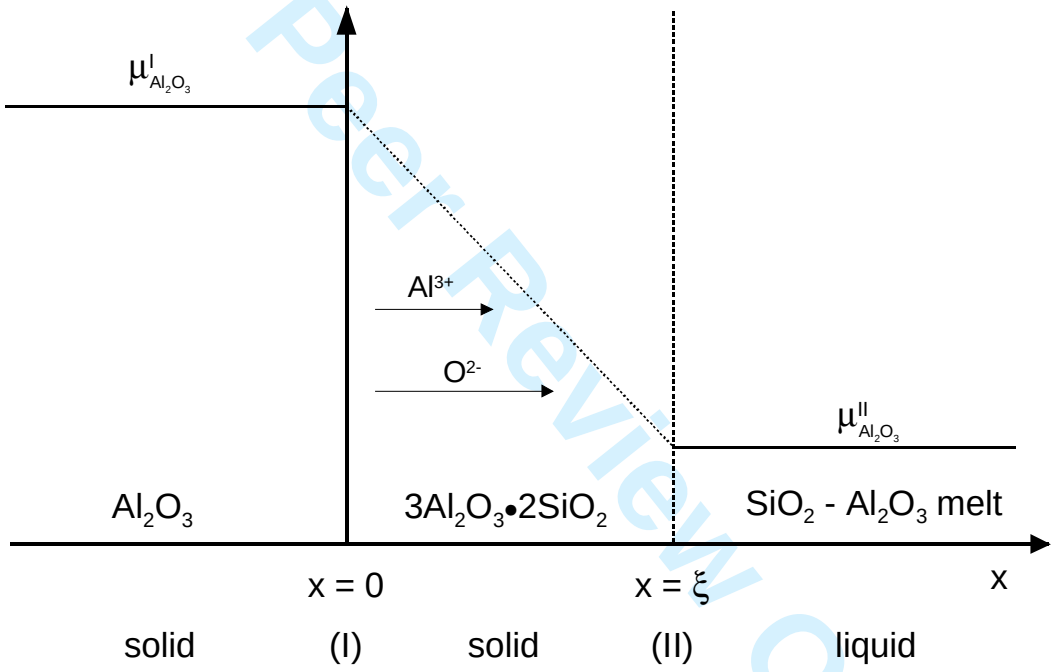

Fig. 2